”Development of ytterbium-doped optical glasses and glassceramics and their response to various treatments”

Mikko Hongisto

THÈSE EN COTUTELLE PRÉSENTÉE

POUR OBTENIR LE GRADE DE

DOCTEUR DE

L'UNIVERSITÉ DE BORDEAUX
ET DE L'UNIVERSITE DE TAMPERE

ÉCOLE DOCTORALE DES SCIENCES CHIMIQUES

SPÉCIALITÉ : PHYSICO-CHIMIE DE LA MATIERE CONDENSEE

Par Mikko Hongisto

Développement de verres et vitrocéramiques dopés ytterbium pour l'optique et réponses sous différents types de traitements

Development of ytterbium-doped optical glasses and glassceramics and their response to various treatments

Sous la direction de : Véronique JUBERA et Laeticia PETIT

Soutenue le 29 Février 2024

Membres du jury :

Mme. PASCUAL FRANCISCO María J.	Chercheuse, Instituto de Cerámica y Vidrio - CSIC	Rapporteure
M. VIANA Bruno	Professeur, PSL University Chimie Paristech	Rapporteur
M. CALVEZ Laurent	Professeur, Université de Rennes 1	Examinateur
Mme JUBERA Véronique	Professeure, Université de Bordeaux	Directrice de thèse
Mme. PETIT Laeticia,	Professeure, Université de Tampere	Directrice de thèse

Membre invité :

M. DANTO Sylvain, Dr	Docteur, Université de Bordeaux	Co-encadrant de thèse

Development of ytterbium-doped optical glasses and glass-ceramics and their response to various treatments

PREFACE

This doctoral thesis, "Development of ytterbium-doped optical glasses and glass-ceramics and their response to various treatments," represents an eventful journey through a cotutelle double-degree program between Tampere University in Finland and Bordeaux University in France during the period of 2019 to 2023. My time was divided between two key research groups: the Photonic Glasses Group at Tampere University's Physics department and the Chemistry and Photonic of Oxide and Fluoride Materials group at the Institut de Chimie de la Matière Condensée de Bordeaux (ICMCB).

Throughout this journey, I had the privilege of being guided by Prof. Laeticia Petit from Tampere University, Prof. Véronique Jubera from Bordeaux University, and Dr. Sylvain Danto, my co-supervisor from Bordeaux. Their persistent support and guidance were invaluable, especially during the challenging final stages of this thesis. This journey would not have been the same without the assistance and collaboration of several colleagues at both institutions. At Tampere University, I am grateful for the contributions of Alexander Veber, Nirajan Ojha, Vilma Lahti, Otto Linros, Iuliia Shestopalova, Turkka Salminen, Jonathan Massera, Sonya Ghanavati, Arnaud Lemiere, Mikko Närhi, Agata Szczodra, and all others who worked alongside me. At Bordeaux, I am thankful for the supportive efforts of Louis Cornet, Shashank Boraiah, Georges El-Dib, Laura Loi, Alexandre Fargues, Gregory Hauss, and Dominique Bernard, as well as all others who contributed to my work.

Beyond the academic sphere, I want to express my deepest gratitude to my friends and family. Their unwavering support, understanding, and encouragement have been my pillars of strength throughout this journey. This thesis, while a significant step in my life, is ultimately a contribution to the broader understanding of ytterbium-doped optical glasses and glass-ceramics. I hope that it will serve as a valuable resource for those who venture into this field in the future.

Mikko Hongisto

ABSTRACT

This dissertation examines methods for modifying the properties of ytterbium-doped glasses through systematic studies of compositional variations and post-processing treatments. New oxyfluorophosphate glass compositions doped with ytterbium ions were developed and characterized to provide fundamental insights on structure-property relationships. Glasses in the $NaPO_3$-Na_2O system with varying fluorine concentrations were prepared and transparent glass-ceramics were obtained by controlled heat treatments. The effects of fluorine content and heat treatments on crystallization behavior and emission spectra were investigated. However, the resultant glasses suffered from hygroscopicity limiting their uses.

To address instability issues, the effects of incorporating aluminum oxide, titanium oxide, and zinc oxide on water absorption overtime was investigated. Results demonstrated that these network-forming oxides could successfully enhance water resistance without hindering the spectroscopic performances of the glass.es However, their crystallization tendencies were impacted. Nevertheless, this established compositional tailoring as an effective approach for strengthening glass connectivity and modifying properties.

Different glass families including phosphate, borosilicate, germanate and tellurite compositions doped with ytterbium were subjected to electron and proton radiation treatments. Their susceptibility to defects formation and their capacity for recovery in response to irradiation were evaluated and compared. Findings identified phosphates and borosilicates as exhibiting the highest initial radiation sensitivity but also greater self-recovery potential upon heat treatment. In contrast, tellurite glasses showed remarkably low defect creation during irradiation highlighting opportunities for radiation resistant materials.

Finally, ytterbium-doped borosilicate glass fibers fabricated with round and rectangular geometries were evaluated for stability in aqueous solution by monitoring the Yb^{3+} emission over time. Results elucidated the significant influence of fiber

design on degradation kinetics, emphasizing that geometry is crucial for controlling resorption behavior tailored to biomedical applications.

Overall, this work advanced fundamental understanding of manipulating Yb^{3+} doped glass-based material performance attributes through thermal, radiation, and compositional modifications. Insights into crystallization, hydrolytic stability improvement, radiation effects, and fiber geometry impacts supported optimization of emissive bandwidth, stability, tolerance, and dissolution profiles. Findings established design strategies and paved the way for further glass-based material progress with applications in photonics, healthcare, and beyond.

RESUME

Cette thèse présente des méthodes visant à modifier les propriétés des verres dopés par des ions ytterbium au travers d'études systématiques de variations de composition et de traitements thermiques.

Dans un premier temps, de nouvelles compositions de verre oxyfluorophosphate dopé à l'ytterbium ont été développées et caractérisées pour une meilleure compréhension fondamentales des relations structure-propriété. Différents taux de fluor ont été introduits au sein de composés du système $NaPO_3$-Na_2O. Cela a conduit à l'obtention de verres et vitrocéramiques transparentes par des traitements thermiques contrôlés. L'analyse thermique a révélé les effets de la teneur en fluor et des traitements thermiques sur le comportement de cristallisation et les spectres d'émission. Cependant, les verres résultants possèdent un caractère hygroscopique, limitant ainsi leurs applications potentielles.

Dans un second temps, les effets de l'incorporation d'oxyde d'aluminium, d'oxyde de titane et d'oxyde de zinc ont été étudiés pour résoudre les problèmes d'instabilité. Les résultats ont démontré que ces oxydes formateurs améliorent la résistance à l'eau sans affecter la réponse spectroscopique du matériau. En revanche, cela modifie le comportement du verre du point de vue de sa cristallisation. On soulignera à ce stade l'impact de la modulation de composition chimique sur la connectivité du verre et la modification de ses propriétés thermiques.

La stabilité sous flux de particules a ensuite été testée. Différentes familles de verres incluant des phosphates, des borosilicates, des germanates et des tellurites dopées par des ions ytterbium, ont été soumises à des traitements d'irradiation par des faisceaux d'électrons ou de protons. Leur susceptibilité à la formation de défauts et leur comportement sous irradiation ont été évalués et comparés. Les résultats ont identifié les phosphates et les borosilicates comme présentant la plus grande sensibilité initiale au flux d'irradiation, mais aussi une plus grande facilité d'effacement, par traitement thermique, des défauts induits. En revanche, les verres tellurites ont montré une forte résistance à la création de défauts, mettant en évidence

leur potentialité en tant que matériaux robustes sous de telles conditions d'irradiation.

Le dernier paramètre étudié dans le cadre de ce travail est la mise en forme du composé vitreux. Des fibres de verre borosilicate dopées par des ions ytterbium, fabriquées avec des géométries rondes et rectangulaires, ont été comparées pour évaluer leur stabilité en milieu aqueux. Ces résultats ont mis en évidence une influence significative de la conception des préformes sur la cinétique de dégradation des fibres. Ceci souligne le fait que leur géométrie est cruciale pour contrôler le comportement de résorption, paramètre de suivi dans le cadre d'applications biomédicales.

Cette étude a fait avancer la compréhension fondamentale des performances de matériaux vitreux de différentes natures au travers de la modulation de compositions chimiques, des variations thermiques, de traitements d'irradiation ou encore de mise en forme. Les effets sur la cristallisation, l'amélioration de la stabilité en milieu aqueux, la génération de défauts et les impacts de la forme ont été analysés au regard la largeur spectrale des émissions, des analyses chimiques et structurales et des profils de dissolution. Les résultats ont permis d'affiner de meilleures stratégies de conception et ont ouvert la voie à de nouveaux progrès applicables aux matériaux vitreux pour des applications en photonique, en santé, et au-delà.

TIIVISTELMÄ

Tämä väitöskirja tutkii menetelmiä ytterbiumilla seostettujen lasien ominaisuuksien muokkaamiseksi systemaattisten koostumuksen vaihteluiden ja jälkikäsittelyjen avulla. Uusia ytterbiumilla seostettuja oksifluorifosfaattilasikoostumuksia, kehitettiin ja karakterisoitiin tarjoamaan perustietoa rakenteen ja ominaisuuksien suhteista. Lasit $NaPO_3$-Na_2O-järjestelmässä, joissa oli vaihteleva fluoripitoisuus, valmistettiin ja lämpötilan säätelyn avulla saatiin aikaan läpinäkyviä lasikeraamisia aineita. Lämpöanalyysi paljasti fluoripitoisuuden ja lämpökäsittelyjen vaikutukset kiteytymiskäyttäytymiseen ja emissiospektreihin. Kuitenkin tuloksena olevat lasit kärsivät hygroskooppisuudesta, mikä rajoitti sovelluksia.

Epävakausongelmien ratkaisemiseksi tutkittiin alumiinioksidin, titaanioksidin ja sinkkioksidin pienien lisäysten vaikutuksia. Tulokset osoittivat, että nämä rakennetta muodostavat oksidit voivat onnistuneesti parantaa vedenkestävyyttä estämättä spektroskooppista suorituskykyä. Kuitenkin kiteytymistaipumukset muuttuivat ratkaisevasti. Tästä huolimatta tämä vahvisti koostumuksen räätälöinnin tehokkaaksi lähestymistavaksi lasin yhteyden vahvistamiseksi ja ominaisuuksien muuttamiseksi.

Eri lasiperheisiin kuuluvia, ytterbiumilla seostettuja fosfaatti-, borosilikaatti-, germanaatti- ja telluriittilaseja, altistettiin elektronien ja protonien säteilylle. Niiden alttius defektien muodostumiselle ja kyky palautua säteilyn vaikutuksesta arvioitiin ja verrattiin. Tulokset osoittivat, että fosfaatit ja borosilikaatit osoittivat suurimman alkuherkkyyden säteilylle, mutta myös suuremman itsepalautumispotentiaalin lämpökäsittelyn jälkeen. Sen sijaan telluriittilasit osoittivat huomattavan alhaisen vikojen muodostumisen, mikä korosti mahdollisuuksia säteilyä kestäville materiaaleille.

Ytterbiumilla seostettuja borosilikaattilasikuituja, pyöreillä ja suorakulmaisilla geometrioilla, arvioitiin vakauden osalta vesiliuoksessa seuraamalla ytterbiumin emissiota ajan myötä. Tulokset valaisivat kuitusuunnittelun merkittävää vaikutusta hajoamiskinetiikkaan, korostaen että rakenne on ratkaiseva resorptiokäyttäytymisen ohjaamisessa biolääketieteellisiin sovelluksiin.

Kaiken kaikkiaan tämä työ edisti perustietoa lasin suorituskykyominaisuuksien manipuloinnista lämpö-, säteily- ja koostumusmuutosten kautta. Oivallukset kiteytymisestä, hydrolyyttisen stabiilisuuden parantamisesta, säteilyn vaikutuksista ja kuitugeometrian vaikutuksista tukivat emissiokaistanleveyden, stabiilisuuden, sietokyvyn ja liukenemisprofiilien optimointia. Tulokset loivat suunnittelustrategioita lasikuitusuunnitteluun ja raivasivat tietä edelleen lasipohjaisten materiaalien edistämiselle muun muassa fotoniikassa ja terveydenhuollossa.

RESUME ELARGI

Les verres sont devenus des matériaux omniprésents qui jouent un rôle important dans un large éventail de technologies et de produits de consommation courante. Leur structure amorphe permet d'envisager des variations presque illimitées de la composition chimique en jouant sur la nature des réactifs oxydes et non oxydes utilisés. Cette flexibilité de composition permet de moduler leurs propriétés physiques et chimiques en fonction des domaines d'applications visés. Parmi eux, les verres dopés par des ions terres rares ont suscité un intérêt considérable dans le domaine de la recherche en photonique. Leurs réponses sur de large domaine de transmission couplées à une facilité de mise en forme permettent en effet d'envisager leur intégration au sein de différents types de dispositifs en tant qu'objets massifs ou fibres et de pourvoir ainsi aux exigences d'une utilisation en télécommunication, en tant que capteurs, milieu à gain pour des lasers, pour de la détection de particules, en imagerie etc. Différents matériaux vitreux tels que les systèmes à base de groupements types phosphate, borate, silicate et germanate, co-dopés par des ions de terres rares comme l'ytterbium, ont démontré un grand potentiel en tant que milieu à gain en vue d'application LASER. Cependant, des facteurs tels qu'une bande passante d'émission limitée, un caractère hygroscopique, une faible conductivité thermique ou encore une mauvaise tenue sous irradiation de forte intensité requiert un travail d'optimisation supplémentaire afin de proposer des composants vitreux à haut potentiel présentant une fiabilité supérieure. Les contraintes technologiques liées à des cahiers des charges de plus en plus exigeants nécessitent donc de poursuivre activement les efforts menés en vue d'améliorer les performances et la durée de vie des technologies basées sur l'emploi de matériaux vitreux.

À l'heure actuelle, seuls les composés de type silicate et quelques compositions exotiques dans les systèmes phosphates, fluorures ou chalcogénures, ont atteint le degré de maturité requis à une commercialisation à grande échelle. On notera toutefois, que certaines compositions autres pourraient offrir des propriétés accrues grâce à une modulation de la composition chimique, à des traitements thermiques contrôlés ou à certains traitements par rayonnement.

Ce travail de doctorat vise à faire progresser la compréhension fondamentale des relations structure-propriété dans des verres dopés par des ions terres rares grâce à une série d'études systématiques portant à la fois sur les effets des variations de composition chimique et sur des méthodes de post-traitement thermique. L'accent est mis sur les systèmes de type oxyfluorophosphate et borosilicate dopés par des ions Yb^{3+}, ce dopage visant à conférer des propriétés d'émission infrarouge aux matériaux. Le contrôle de la chimie du verre, de sa micro- et macro-structure au travers des états de cristallisation et de nouvelles géométries sont autant de paramètres qui ont été mis en œuvre. En parallèle, des variables telles que la teneur en fluor, l'ajout d'oxydes formateurs et modificateurs de réseaux, l'exposition à différents rayonnements ont été méthodiquement modulées. Les matériaux ainsi pensés sont caractérisés du point de vue de leurs spectres de photoluminescence, de leur comportement thermique et leur tendance à la cristallisation, de la cinétique de dissolution en milieu aqueux et de leur tenue aux rayonnements de protons et d'électrons. Concernant ce dernier point, une étude de la réponse à une telle exposition permet d'apporter des éléments de réponse concernant la compréhension des matériaux soumis à des doses élevées de radiations comme ce peut être le cas dans le domaine de la santé, au sein des accélérateurs de particules ou dans l'espace. L'objectif est de mieux appréhender la stabilisation de centres colorés, de défauts à l'origine d'une dégradation de la réponse optique (pertes de transmission du matériau, variation d'indice etc.). Pour compléter ces études, la dégradation de fibres de verre borosilicaté bioactives dopées par des ions ytterbium en milieu aqueux est enregistrée. Au-delà de l'impact de la composition chimique, c'est l'influence de la géométrie de la fibre qui est étudiée. Un comparatif entre fibre cylindrique et rectangulaire est donc proposé.

Grâce à des études approfondies faisant appel à une approche multidisciplinaire, de nouvelles stratégies et de nouveaux principes devraient émerger pour optimiser des paramètres critiques tels que les propriétés de luminescence, la stabilité au regard du milieu, la stabilité sous rayonnement et la cinétique de dissolution des verres dopés par des ions terres rares. L'objectif principal est de proposer des pistes afin de repousser les limites actuelles d'intégration des composés vitreux.

1. Définition des objectifs de recherche

Différentes problématiques ont été formulées dans le cadre de ce travail.

i. La composition chimique

- Comment l'ajout de fluor affecte-t-il la cristallisation d'un verre de type phosphate dopé par des ions Yb^{3+}?

- Quels sont les effets des traitements thermiques contrôlés sur la cristallisation et les spectres d'émission?

- Comment l'incorporation d'oxydes tels que Al_2O_3, ZnO et TiO_2 dans ces matrices vitreuses influence-t-elle la connectivité du réseau et la résistance du verre à l'absorption d'eau ? Y-a-t-il un effet sur les mécanismes de nucléation et de croissance de particules cristallines?

- Peut-on optimiser la résistance à l'eau tout en conservant les propriétés mécaniques ou optiques initiales?

Les **Publications 1 et 2** apportent des réponses à ces questions.

ii. La tenue à l'irradiation

- Comment les différentes familles de verre de type silicate, phosphate, borate ou tellurite se comportent-elles au regard de leur tendance à la formation de centres colorés et de changements microstructuraux induits par rayonnement?

- Peut-on identifier des compositions de verre présentant des tolérances au rayonnement élevées/faibles?

- Comment les techniques de post-traitement comme un traitement thermique influencent-elles l'effacement des défauts?

Ces questions ont été abordées de façon élargie dans **une revue de papiers** et dans le cadre du travail associé à la **Publication 3.**

iii. La tenue en milieu aqueux et effets de géométrie

- Comment la géométrie du verre et les conditions de fabrication influent-elles sur la cinétique de dégradation des fibres de type borosilicate bioactif en milieu aqueux?

- Les propriétés spectroscopiques Yb^{3+} peuvent-elles être utilisées pour suivre la dégradation de la fibre en milieu aqueux ?

Ces points sont argumentés au sein de la **Publication 4**.

2. Déroulé du manuscrit

Cette thèse est structurée comme suit : après une brève introduction (Chapitre 1), le Chapitre 2 présente les concepts généraux liés aux matériaux vitreux et vitrocéramiques en se centrant sur le dopage de ces derniers par des ions ytterbium. Un état actuel succinct de la recherche sur les sujets d'intérêt conclut cette partie. Ceci inclut notamment des informations sur la fibre optique et sa fabrication via différentes méthodes.

Le Chapitre 3 liste les différentes conditions expérimentales de synthèse des matériaux vitreux et les caractérisations mises en œuvre.

L'ensemble des résultats expérimentaux et analyses sont reportés dans le Chapitre 4. Ce dernier est divisée en trois sous-sections illustrant les trois problématiques précédemment citées (composition chimique, effet d'irradiation et de géométrie en milieux aqueux).

Le document se termine par une conclusion générale suivi des sources bibliographiques sur lesquelles s'appuient l'argumentaire de la thèse.

3. Principaux résultats et discussions

i. La composition chimique

De nouveaux verres oxyfluorophosphates dopés par des ions Yb^{3+} et des vitrocéramiques ont été synthétisés et caractérisés. Une vitrocéramique transparente du matériau sans fluor a été obtenue suite à un traitement thermique contrôlé. Le

travail d'incorporation de l'halogène permet de travailler sur la largeur de la fenêtre de transmission du matériau aussi bien que sur la répartition spectrale en émission de l'ion terre rare. De faibles modulations sont ainsi observées. Cependant, ces compositions vitreuses se sont avérées hygroscopiques limitant de fait, leur utilisation en milieu humide non contrôlé.

La réponse adoptée a été la suivante : des oxydes d'aluminium, de titane et de zinc ont été ajoutés à la composition nominale du verre afin améliorer sa résistance à l'eau. Les résultats se sont avérés prometteurs. Les changements de composition entraînent des modifications des mécanismes de nucléation, croissance et donc de résistance thermique. L'incorporation d'Al_2O_3 et de TiO_2 conduit non seulement à une résistance accrue à la cristallisation, mais empêche également une cristallisation massive. Ces deux oxydes sont donc acteurs de la consolidation du réseau vitreux. En revanche, les tentatives d'incorporation d'oxyde de Zinc aboutissent à une résistance moindre à la cristallisation des compositions visées. L'ajout de zinc sous forme d'oxyde lors du processus de synthèse n'est donc pas une alternative envisageable si l'on souhaite un renforcement de la tenue au traitement thermique des matériaux.

La modulation chimique des compositions initiales des verres type oxyfluorophosphate dopés Yb^{3+} pointe des voies d'amélioration des propriétés thermiques et spectroscopiques mais aussi d'une meilleure résistance à l'humidité du milieu environnement.

ii. La tenue sous irradiation

L'effet des traitements par rayonnement protonique ou électronique sur les propriétés optiques et spectroscopiques de divers verres dopés Yb^{3+} est examiné. Les résultats mettent en évidence des comportements différents en fonction de la nature des réseaux vitreux testés. Les composés de type phosphate, borosilicate s'avèrent être les plus sensibles. On observe que les irradiations appliquées modifient significativement les propriétés d'absorption dans l'ultraviolet et le visible en créant de nouveaux défauts, ce qui a une incidence notable sur les caractéristiques optiques de ces matériaux. A titre d'exemple, l'intensité d'émission des ions Yb^{3+}, indicateur de la performance LASER potentielle, diminue dans tous les verres irradiés excepté le verre de type tellurite qui présente une excellente stabilité. On note cependant, que

la stabilisation des défauts est réversible. En effet, des études menées sur les composés irradiés, trois mois après les traitements, montrent une ré-augmentation spontanée et significative du coefficient d'absorption dans le domaine des longueurs d'onde de 250 à 500 nm. Ceci illustre une réduction substantielle du nombre de défauts photo-induits sous faisceau de protons ou d'électrons. Un traitement thermique approprié conduit de la même façon à une « réparation chimique » de la matrice vitreuse par effacement des défauts, l'intensité d'émission retrouvant son niveau initial.

Les verres d'oxyde de métaux lourds (type germanate, tellurite) sont les plus robustes sous irradiation et présentent finalement les meilleures propriétés. Il faut cependant garder à l'esprit les contraintes d'élaboration de ces matériaux au regard de leur composition chimique (coût, stabilité, température et atmosphère de synthèse …) et du domaine d'applications envisagé. Une étude plus approfondie de ces changements optiques observés au sein des matériaux testés pourrait mener à des progrès quant à la conception et l'application de matériaux résistants aux radiations.

iii La tenue en milieu aqueux et les effets de géométrie

Cette dernière étude vise à étudier la stabilité des verres dopés par des ions Yb^{3+} en milieu aqueux. Pour se faire, des fibres bioactives cylindriques et rectangulaires ont été fabriquées à partir de préformes vitreuses complexes de type borosilicate dopées et non dopées constituant respectivement le cœur et la gaine de la fibre. Un ensemble de caractérisations permet de déterminer les propriétés physico-chimiques, de photoluminescentes et de dissolution des fibres. Ces dernières présentent une excellente qualité à l'interface cœur/gaine avec une diffusion limitée des ions ytterbium du noyau vers la gaine comme illustré au travers d'une cartographie de microluminescence. Ce confinement des espèces optiquement actives est crucial pour les applications photoniques.

Malgré des variations mineures du rapport de diamètre des fibres cylindriques dues aux imperfections de la méthode de fabrication, ces fibres multimodes se sont avérées utiles à des fins de recherche. Le profil de section transversale externe de la fibre influence de manière significative leur comportement de biodégradation. Ces observations soulignent l'impact de la conception de la fibre sur la fonctionnalité du matériau résultant. Les fibres rectangulaires présentent en effet des pertes élevées

(environ 30 dB/m à 800 nm) et une dégradation accélérée comparativement aux fibres cylindriques, en raison des contraintes de traction résiduelles induites lors du processus de fibrage. Une analyse de la concentration de ces dernières a révélé la présence de contraintes de traction localisées aux coins externes rectangulaires des fibres, affectant leur réactivité chimique et leur intégrité structurelle. Ces résultats suggèrent l'importance de la géométrie dans le comportement de dégradation des fibres et soulignent le nécessité d'une conception et d'une fabrication soignées pour optimiser la cinétique de biodégradation spécifique à une application biomédicale (délivrance de médicaments…).

4. Conclusion et perspectives

Pour conclure, ce travail propose une étude sur la modification des propriétés des composés vitreux dopés par des ions Yb^{3+}, à travers des variations de composition, de traitements thermiques ou par rayonnement ainsi que par immersion en milieu aqueux. De nouveaux verres/vitrocéramique type oxyfluorophosphate dopés Yb^{3+} ont été développés et caractérisés pour obtenir des informations fondamentales sur la cristallisation. Cette étude fournit également des informations sur la résistance aux défauts en fonction de la nature du réseau et sur le développement de nouvelles fibres bioactives, dont l'émission pourrait être utilisée pour suivre la dissolution de la fibre dans le milieu aqueux.

À partir des résultats obtenus, des pistes d'optimisation peuvent être envisagées :

• Concernant les vitrocéramiques transparentes dopées par des ions Yb^{3+}, de futurs travaux pourraient explorer les aspects de « scale-up » de façon à les produire à plus grande échelle. Une production sur des volumes plus conséquents permettrait d'effectuer une caractérisation plus fine et quantifiable en vue d'une ingénierie adaptée aux dispositifs LASER / amplificateurs.

• L'incorporation d'oxydes formateurs de réseau améliore la stabilité de la matrice vitreuse étudiée mais influence également sa tenue à la cristallisation. Un examen plus approfondi des relations structure-propriétés pourrait fournir des lignes directrices de conception afin d'optimiser les deux attributs simultanément.

• La tenue au flux est fortement dépendante de la nature du réseau vitreux. Des études complémentaires pourraient se concentrer sur le contrôle des défauts photo-

induits via l'incorporation de métaux alcalins ou alcalino-terreux modificateurs de réseaux tels que le potassium ou le baryum. En complément, une meilleure compréhension des mécanismes d'extinction de luminescence des ions de Yb^{3+} observée au sein des composés type germanate ainsi que de la résistance des verres type tellurite pourrait être utile à l'amélioration des systèmes.

• La géométrie des fibres a un impact significatif sur le comportement de biodégradation des verres type borosilicate. Une amélioration des paramètres de conception des préformes et des conditions de tirage devraient permettre une réduction de la concentration des contraintes, notamment celles détectées aux coins externes des fibres rectangulaires. L'originalité de la mise en forme planaire de ces objets reste toutefois intéressante pour le développement de fibres de conceptions uniques pouvant s'intégrer au sein de dispositifs. Le contrôle de la cinétique de biodégradation présente lui un intérêt potentiel dans les thérapies biomédicales.

Dans l'ensemble, cette étude contribue à une meilleure compréhension fondamentale sur la façon dont les modifications de composition et les processus thermiques / de rayonnement peuvent moduler les paramètres de performance des matériaux vitreux dopés par des ions Yb^{3+}. Les résultats obtenus illustrent de nouvelles stratégies et de nouveaux principes de conception pour améliorer les propriétés optiques souhaitées telles que la largeur spectrale en absorption et en émission, la stabilité sous rayonnement et les profils de dissolution. Cette démarche entre dans un processus d'amélioration continue des matériaux et d'utilisation plus large des composés vitreux pour des applications polyvalentes. Ce travail fournit une base visant à susciter de nouvelles recherches afin de repousser les limites d'utilisation des matériaux vitreux pour des applications dans les domaines de la photonique, de la santé, de la détection des radiations et au-delà.

CONTENTS

List of Figures

List of Tables

ABBREVIATIONS

CVD - Chemical Vapor Deposition
EDS - Energy dispersive X-ray spectroscopy
FTIR - Fourier transform infrared spectroscopy
HA – Hydroxyapatite
HT - Heat treatment
HMO - Heavy metal oxide
ICP-OES - Inductively coupled plasma optical emission spectrometry
IR – Infrared
MCVD - Modified Chemical Vapor Deposition
MIR - Mid-infrared
NBOHC - Non-bridging oxygen hole centers
NIR - Near-infrared
ODC - Oxygen-deficient center
OHC - oxygen hole centers
POHC - Phosphorus oxygen hole center
PDT - Photodynamic therapy
Qn - Glass structure notation
SBF - Simulated body fluid
SEM - Scanning electron microscopy
SCC - Stress corrosion cracking
STH - Self-trapped hole
VAD - Vapor Axial Deposition
XRD - X-ray diffraction

LIST OF PUBLICATIONS

Publication 1: M. Hongisto, A. Veber, N. G. Boetti, S. Danto, V. Jubera, and L. Petit, "Transparent Yb3+ doped phosphate glass-ceramics," *Ceram Int*, vol. 46, no. 16, pp. 26317–26325, Nov. 2020, doi: 10.1016/J.CERAMINT.2020.01.121.

Publication 2: M. Hongisto, O. Linros, S. Danto, V. Jubera, and L. Petit, "Impact of Al2O3, TiO2 and ZnO addition on the crystallization of Yb3+ doped phosphate glass-ceramic," *Mater Res Bull*, vol. 157, p. 112032, Jan. 2023, doi: 10.1016/J.MATERRESBULL.2022.112032.

Publication 3: M. Hongisto *et al.*, "Response of Various Yb3+-Doped Oxide Glasses to Different Radiation Treatments," *Materials*, vol. 15, no. 9, p. 3162, May 2022, doi: 10.3390/MA15093162/S1.

Publication 4: M. Hongisto *et al.*, "Characterization of biodegradable core–clad borosilicate glass fibers with round and rectangular cross-section," *Journal of the American Ceramic Society*, Jul. 2023, doi: 10.1111/JACE.19304.

1 INTRODUCTION

Glasses have become ubiquitous materials that play important roles across a wide range of technologies and everyday consumer products. Their amorphous structure allows for nearly limitless variations in chemical composition through introduction of various oxide and non-oxide components. This exceptional compositional flexibility has enabled glasses to be tailored with a diverse array of physical and chemical properties. Rare earth-doped glasses have attracted substantial research interest due to their luminescent characteristics, which support applications such as lasers, fiber amplifiers, bioimaging labels, and more. However, continued advancements are still needed to address pressing challenges that may limit performance and lifetime of these glass-based technologies.

Different glass families, such as phosphate, borate, silicate, and germanate glass systems co-doped with rare earth ions like ytterbium have demonstrated great potential as gain media and laser hosts. However, factors including limited emission bandwidth, deficient hydrolytic and thermal stability, and degradation under high intensity radiation benefit from further optimization in providing their full potential in high-power lasers, amplifiers, and other devices requiring reliability over extended usage. Currently, only the silicates and few phosphates have reached the stage of widespread commercial adoption, with niche applications in chalcogenide and fluoride glasses. Alternative compositions could offer improved properties through compositional tailoring and thermal or radiation treatments to "tune" the material on a fundamental level.

This dissertation aims to significantly advance the fundamental understanding of structure-property relationships in rare earth-doped glasses through a series of systematic studies examining the effects of compositional variations and post-processing methods on various glass properties. A focus is placed on ytterbium-doped oxyfluorophosphate and borosilicate glass systems, which show promise as gain media and whose performance attributes can likely be further enhanced through controlled manipulation of glass chemistry, microstructure (crystallization) and macrostructure (novel fiber geometries). Variables such as fluoride content,

additions of network-forming and -modifying oxides, and thermal or radiation processing conditions are methodically varied. The resulting impacts on critical material traits including photoluminescence emission spectra, crystallization behavior, hydrolytic dissolution kinetics, and radiation effects are thoroughly investigated in this thesis.

Beyond ytterbium-doped glasses, the dissertation also explores responses of different glass families including phosphate, borate, tellurite, and silicate compositions to radiation exposures through electron and proton beam treatments. Such investigations provide a foundation for developing radiation-resistant glass-based technologies suitable for applications involving high radiation doses encountered in healthcare, spectroscopy, accelerators, and space. This research helps one to understand the degradation seen in high power lasers, known as photodarkening. In the last part of the thesis, bioactive borosilicate glass fibers doped with ytterbium are developed with distinct round and rectangular geometries to gain insights on fiber shape impacts on degradation performance in aqueous medium.

Through these in-depth investigations employing a multidisciplinary approach, new strategies and principles are expected to emerge for optimizing critical attributes such as luminescence properties, environmental stability, radiation tolerance, and dissolution kinetics in rare earth-doped glasses. The enhanced understanding will support continued progress and broader utilization of glass-based materials for applications in photonics, healthcare, radiation detection, and more. The overarching goal is to lay groundwork inspiring future efforts to push boundaries of glass-based materials developed for various applications related to photonics.

1.1 Research objects

The following research questions were determined for this thesis to answer:

1. How does the addition of fluorine affect Yb^{3+} -doped phosphate glass crystallization? What effects do controlled heat treatments have on crystallization and emission spectra of the Yb^{3+} -doped oxyfluorophosphate glasses? How does the incorporation of Al_2O_3, ZnO and/or TiO_2 in this glass network influence the glass network connectivity and the resistance of the glass to water absorption? How would it change its nucleation and

growth mechanism? Can water resistance be optimized without compromising other attributes? These questions are addressed in **Publications 1 and 2**.

2. How do different glass families (silicates, phosphates, borate, tellurite, etc.) compare in their susceptibility to radiation-induced formation of color centers and microstructural changes? Can glass compositions be identified so that the glass exhibit tailored (high/low) radiation tolerances? How do post-processing techniques like thermal treatment influence defect recovery? These questions are discussed in **Publication 3**
3. How does glass geometry and fabrication conditions impact degradation kinetics of ytterbium-doped bioactive borosilicate fibers in aqueous medium? Can the Yb^{3+} spectroscopic properties be used to track the degradation of the fiber in aqueous medium? These questions are addressed in **Publication 4**.

1.2 Structure of the thesis

This thesis is structured as follow:

Chapter 2 first introduces the relevant concepts and ideas related to the Yb^{3+} doped glass and glass-ceramic, main materials of investigation, followed by the current state of the art of research in the topics of interest. Glasses and glass-ceramics are introduced, along with their key features and differences. Finally, the definition of optical fiber, its manufacturing process via various methods and current research are discussed. A separate subchapter explains the features of biophotonic fibers.

Chapter 3 provides information on glass manufacturing, processing along with fiber fabrication. Subsequently, the various experiments performed are introduced.

Chapter 4 discusses the results of the experiments and how the most important questions are answered based on the obtained data. The section is divided into three subchapters, each focusing on certain aspects of the research.

Chapter 5 provides the main conclusions and discusses potential future areas of research based on the obtained results.

2 BACKGROUND

2.1 Glasses

2.1.1 Theory of glass formation

Glasses, classified as amorphous solids, differ from crystalline ceramics in their absence of long-range periodic structure. A distinguishing characteristic of glasses is the glass transition, a phenomenon during which the material transitions between a supercooled liquid and an amorphous solid state, or vice versa.[1]

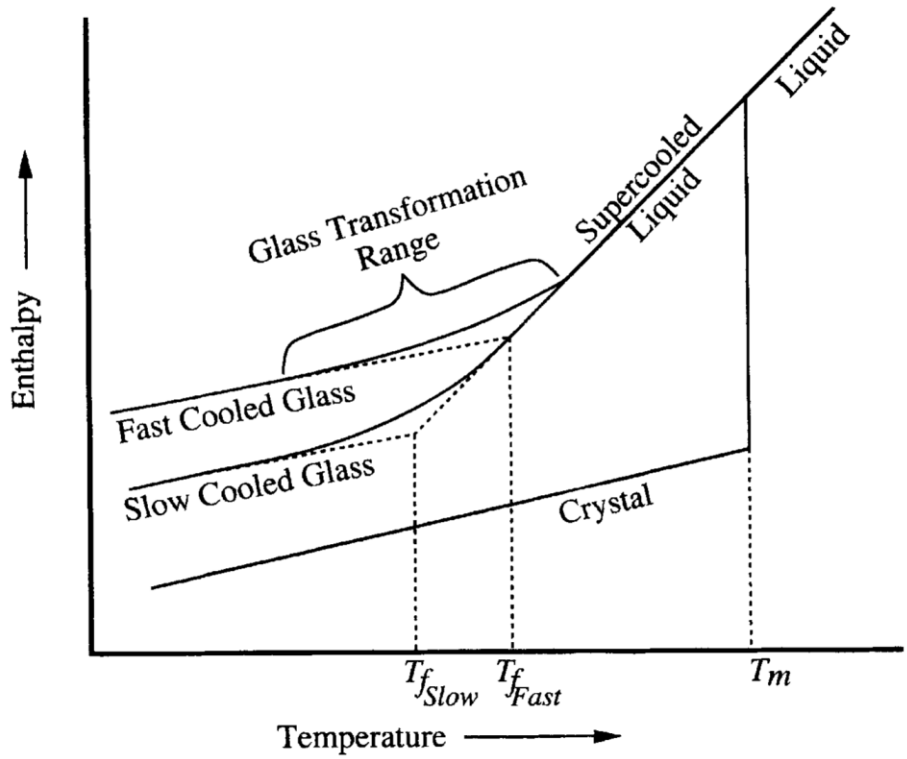

Figure 1. Temperature-Enthalpy curve of glass and crystal.[1]

Figure 1 shows the temperature-enthalpy curves for both the glass and crystal during the cooling process from high temperatures. The enthalpy, a measure of the total energy of the material, decreases as the temperature drops. Unlike crystals that encounter a discrete phase change when the atoms rearrange themselves into a well-ordered crystalline lattice, glasses transition smoothly from liquid to solid. [1] Glasses undergo a glass transition during cooling, where they transform from a liquid to an amorphous solid state. The cooling rate plays a vital role in this transition, as it must be sufficiently fast to prevent the supercooled liquid from crystallizing. If the cooling rate is sufficient, the supercooled liquid can reach the glass transition, where the viscosity has increased substantially, hindering the rearrangement of atoms into a crystalline lattice. As a result, the glassy structure remains amorphous, "freezing" the liquid-like structure into a solid. Therefore, the atomic arrangement in the glass network resembles that of liquids, characterized by the absence of long-range periodic order. [1]

Many compounds, including metals, can yield glasses when subjected to a sufficiently rapid cooling rate. According to Zachariasen, glass constituents can be categorized into three types: network formers, network modifiers, and intermediates.[2]

- Network formers, such as boron, silicon, germanium, and phosphorus oxides, constitute the glass's structural backbone and can independently form glasses.

- Network modifiers are employed to modify the glass structure, affecting properties like the glass transition temperature, chemical resistance, and refractive index, for example. Common modifiers include alkali and alkaline earth oxides.

- Intermediates, like metal oxides such as aluminum and titanium oxides, bond strongly to network formers and become part of the network but cannot form a network on their own.[1], [2]

2.1.2 Glass systems

Glasses can be categorized into oxide and non-oxide glasses. The non-oxide glasses are glasses that do not contain oxygen nor oxides. Examples of such non-oxide

glasses are chalcogenide and fluoride glasses that are common in mid and long-infrared applications, such as sensors and imaging. Chalcogenide glasses are made from S, Se and/or Te while the fluoride glasses contain F. Here the focus is on oxide-based glasses. The most common and well-known class of oxide glasses contains the silica glasses. However, phosphate, germanate and tellurite glasses, among others, do exist and currently serve some niche uses such as laser glasses for phosphates and radiation shielding for the heavy metal glasses such as germanate and tellurite glasses. The glasses of investigation were:

- **Borosilicate Glasses:** Known for their bioactive and biodegradable properties, these glasses can degrade in a controlled manner, making them ideal material for specific biomedical applications such as biomedical devices.[3] The most recognized and industrially produced bioactive glasses is the 45S5 Bioglass, 45 wt% SiO_2, 24.5 wt% Na_2O, 24.5 wt% CaO, and 6 wt% P_2O_5. Its outstanding ability to form a hydroxyapatite layer upon immersion in body fluids underpins its significant bioactivity.[4] Another noteworthy type is S53P4, which consists of 53 wt% SiO_2, 23 wt% Na_2O, 20 wt% CaO, and 4 wt% P_2O_5. S53P4 is renowned for its antimicrobial properties, particularly against biofilm formation, adding another layer of bioactivity to its profile. [5] The 13-93 glass has a more complex formulation that consists of 53 wt% SiO_2, 20 wt% CaO, 6 wt% Na_2O, 4 wt% K_2O, 12 wt% MgO, and 5 wt% P_2O_5, a composition that exhibits enhanced mechanical properties and bioactivity. [5]

- **Germanate and Tellurite Glasses:** As heavy metal oxide glasses, they possess unique optical properties that make them suitable for a variety of photonic applications. They both possess wide transmission windows from visible to the mid-infrared region. They have low maximum phonon energies (800-900 cm^{-1} vs. 1100-1200 cm^{-1}), making them attractive rare-earth hosts for rare earth ions as low phonon energies increase the RE emission quantum efficiency. [6]–[9]

- **Phosphates:** Sodium oxyfluorophosphate glasses were selected based on previous research that demonstrated their potential to form transparent glass ceramics in a Er^{3+}-doped $NaPO_3$-CaF_2 system. [10] However, they are believed to be highly sensitive to water absorption, raising concerns about their chemical durability over time. The sodium phosphate glass system can be modified for better resistance against water absorption for example by adding modifier ions, such as aluminum oxide, [11]–[13] titanium oxide, and [14]–[19] and zinc oxide

[20]–[24]. For example, aluminum oxide can be added to enhance chemical durability, mechanical properties, and thermal stability of the phosphate glass [11]–[13]. Primarily, the contributions of aluminum oxide to glass modification are underpinned by the changes it induces on the glass structure due to the formation of Al-O-P and Al-O-Al linkages on phosphate glasses, augmenting the resilience of the glass structure. [11]–[13] These linkages can be used to increase the glass resistance to hydrolytic attack, thereby reducing possibility of stress corrosion cracking. Such effects can be directly attributed to the reduction of non-bridging oxygen atoms and the concomitant reinforcement of the glass network, contributing to heightened resilience against crack initiation and propagation in both stress and corrosive conditions. [11]–[13] Titanium dioxide offers similar enhancements in the mechanical, thermal, and optical properties when added in phosphate glass matrix. The integration of titanium ions within the glass network, through the formation of Ti-O-P and Ti-O-Ti bonds in phosphate glass, was reported to lead to a more rigid glass structure and thereby improved thermal stability. [11]–[13] Similarly, the introduction of TiO_2 also enhances the glass's resistance to hydrolytic attack also due to the reduction in the number of non-bridging oxygen atoms leading to the cross-linking of the glass network. Thus, the modified glass demonstrates increased resilience to crack initiation and propagation under challenging conditions such as stress and corrosive environments. Additionally, titanium dioxide acts as a potent nucleating agent, accelerating nuclei formation in several glass systems. [14]–[19] Finally, zinc oxide has shown promising effects on the thermal stability, chemical durability, and mechanical properties of glass ceramics. The introduction of zinc oxide has been linked to a substantial increase in both the glass transition and crystallization temperatures. The presence of zinc ions within the phosphate glass network is thought to disrupt phosphate chains and to form phosphate dimers, i.e., joining chains togethers, resulting in a denser network. This densification enhances the hydrolytic resistance of phosphate glasses, primarily by impeding the diffusion of water into the glass structure [18]–[22]. Nevertheless, the beneficial effects of zinc oxide are contingent on the specific glass composition and the concentration of zinc oxide: high zinc oxide concentrations may yield less optimal glass structures, leading to increased tendency for stress corrosion cracking. [20]–[24]

2.1.3 Glass for lasing applications

One of cores of the photonics cores is the lasing action, that is Light Amplification by Stimulated Emission of Radiation (LASER), or in other words, phase sensitive amplification of light in matter. The lasing process can be understood by examining three key steps: absorption, spontaneous emission, and stimulated emission, These processes are illustrated in Figure 2.

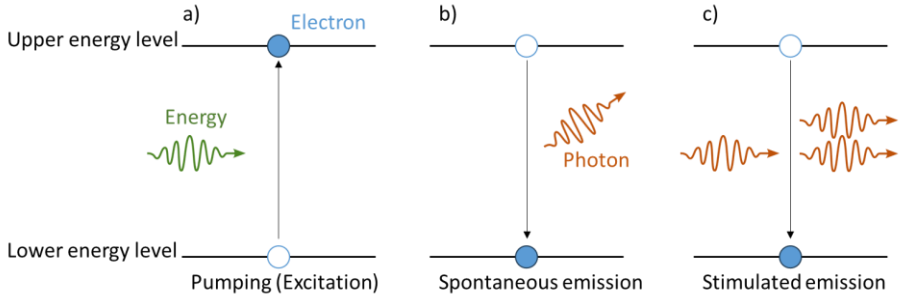

Figure 2. Schematic diagram of the key steps, excitation (a), spontaneous emission (b) and stimulated emission (c), in a lasing process

Excitation: The initial stage of the lasing process begins with the absorption of a photon by an atom or ion, which causes an electron to be excited to a higher energy state in a process colloquially known as pumping. The absorbed photon must have the appropriate energy to facilitate this transition.

Spontaneous Emission: Following the absorption process, the excited electron will eventually return to its initial energy state. When this occurs, a photon is emitted in a process known as spontaneous random emission.

Stimulated Emission: If a photon with similar energy to the emitted photon encounters the excited atom or ion, it can trigger a process called stimulated emission. In this process, the excited electron is stimulated to decay back to its initial energy state, and an identical photon is emitted in the same direction as the incident photon, resulting in coherent light amplification.

The generation of lasing properties requires a specific energetic configuration. During the relaxation process, electrons can be stored in an intermediary excited state (level 3) level. When this excited level (level 3) is more strongly populated than the lower-lying level (or ground state, level 1), the population inversion threshold is reached. To fulfil this condition, the lifetime of the intermediary level (level 3) must

be superior to that of the excited state (level 2). The excited state (level 2) preferentially decays to the intermediary level (level 3) instead of the ground level (level 1). One can describe two main types of lasing configurations, a three-level (Figure 3a) and a four-level system (Figure 3b). With the four-level system, the lasing occurs between two intermediate levels (levels 3, 4).

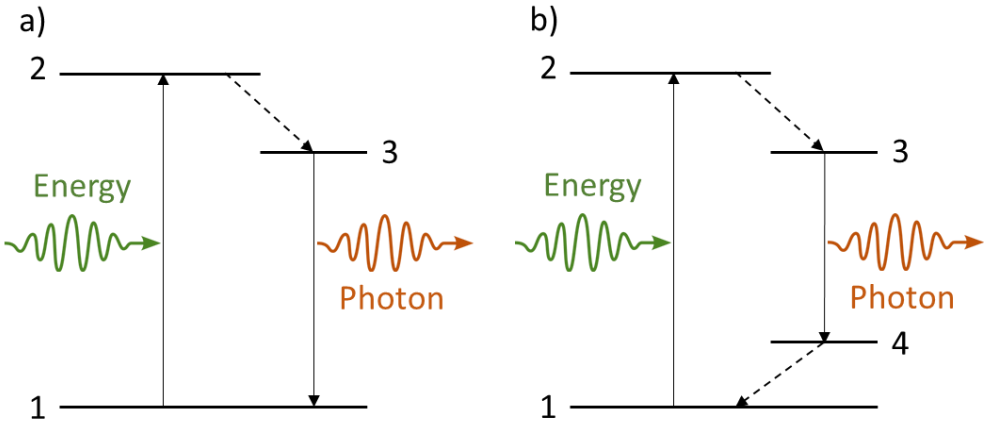

Figure 3. Schematic diagram of a three-level (a) and a four-level (b) lasing system.

Consequently, because of their specific and complex energy diagram, lasing in glasses, can be obtained easily withe rare earth elements, such as Er^{3+}, Tm^{3+}, Pr^{3+}, Ho^{3+} and Yb^{3+}, seen in Figure 4.Figure 4.

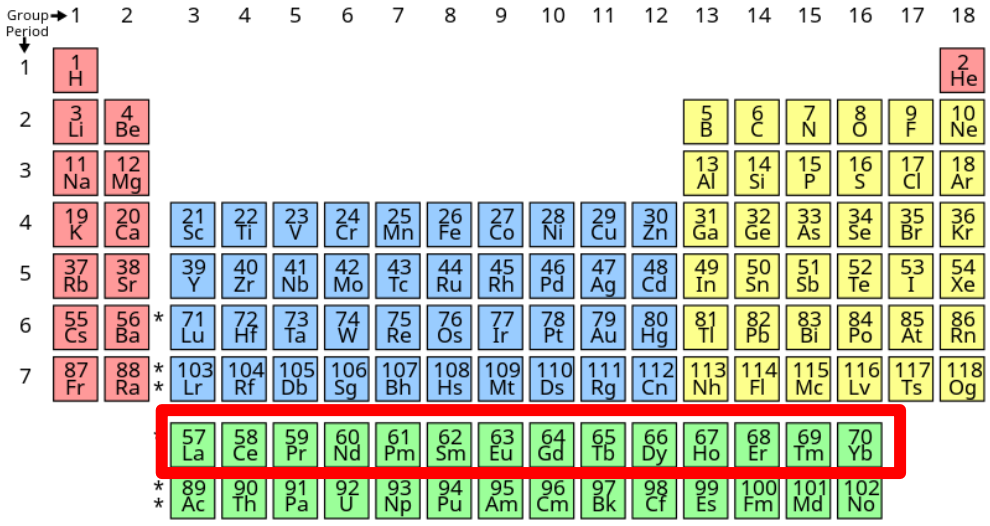

Figure 4. Periodic table with the potential lasing rare earth elements highlighted [25]

2.1.4 Glass for biomedical applications

Glass composition can be tailored so that the glass finds uses in biomedical applications. The materials can be classified into the following categories based on their response. **Non-biocompatible materials** are composed of cytotoxic materials. This group encompasses materials that kill their surrounding tissue. Examples of substances in this group are Pb or As. There are also carcinogenic materials, which do not kill the surrounding tissue but promote the growth of tumors, substances such as Cadmium or Benzene, belong to this group. On the contrary there are **biocompatible materials,** which include:

- **Bioinert materials** do not show any kind of reaction from the body after the initial recovery, or their response is too negligible to be significant. For example, titanium is a bioinert material.

- **Bioactive materials** are materials that stimulate a specific, controlled reaction from the tissue they encounter. Commonly, these materials exhibit attributes such as biosorption and osseointegration. Bioactive glasses, which are both osteoconductive and osteoinductive, are defined as substances that trigger particular surface reactions, resulting in the creation of a layer similar to hydroxyapatite (HA) once they have been implanted into the body. HA is a particular type of phosphate mineral with a distinct ratio of components ($Ca_{10}(PO_4)_6(OH)_2$). However, it can refer to any apatite calcium phosphate that shares significant structural and compositional similarities with HA, typically varying from the ideal stoichiometric composition. The formation of HA-like layer can form bonds with both soft and hard tissues at the same time. A material's ability to form this HA-like layer after being immersed in simulated body fluid (SBF) is often considered as a sign of the material bioactive response. Furthermore, this test of immersion in SBF could potentially indicate the material's bioactive capabilities in a live organism.[4], [5], [26], [27] The composition of bioactive glasses can be tailored to achieve specific properties and functionalities. For instance, by altering the ratio of network formers and modifiers, the dissolution rate and bioactivity of these materials can be controlled, enabling their use in a wide array of applications, from bone grafts and tissue scaffolds to drug delivery systems and coatings for dental implants. The introduction of trace elements such as strontium, zinc, and copper into the

glass composition can impart additional biological functions, including angiogenesis, antimicrobial activity, and anti-inflammatory properties.[4], [5] The materials studied in **Publication 4** belong to this category.

2.2 Glass-ceramics

2.2.1 Nucleation and growth theory

Glasses, akin to diamonds, can be classified as metastable materials. The principle of metastability can be visualized, for instance, in Figure 1, wherein the lower enthalpy state of crystals compared to glasses is depicted, symbolizing the higher stability of atomic arrangements within the crystalline structure. It is possible to transform glasses into a state exhibiting higher crystallinity. This resultant material, referred to as a glass-ceramic, possesses unique properties owing to its constitution. Glass-ceramics represent a novel and distinctive category of materials, situated at the interface between the domains of glasses and ceramics.[28]

Figure 1 Figure 5. shows the structural differences between amorphous glasses, crystalline ceramics, and glass-ceramics. Glass-ceramics are composite materials, constituted by a complex blend of glassy and crystalline components. Over recent years, glass-ceramics have garnered significant interest, particularly within the photonics domain, due to their potential to offer a range of properties that are difficult, if not impossible, to achieve with conventional glasses or ceramics alone. These include enhanced mechanical strength, thermal stability, optical properties, and chemical durability[28]. Despite these advantages, engineering glass-ceramics involves a certain degree of challenge, mainly related to controlling the size and distribution of the crystalline phase. This is crucial since these parameters profoundly influence the resultant properties of the material.[28]

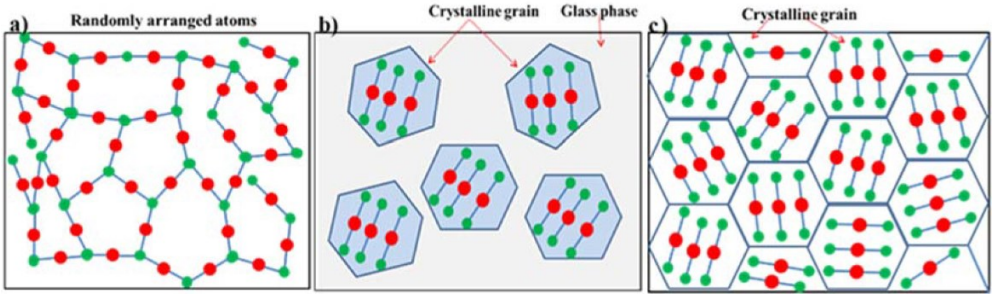

Figure 5. Schematic diagram of glassy structure (a), glass-ceramic (b), and crystalline (c) material.[29]

Glass-ceramics are typically generated through the controlled crystallization of the glass, involving heat treatment to induce crystal growth within the glass matrix. This process can be broadly divided into two stages: nucleation and crystal growth.

- **Nucleation:** The formation of glass-ceramics begins with the generation of nuclei by heat-treating the glass at specific temperatures. To form nuclei, a thermodynamic barrier, represented in Figure 6a, must be overcome. In this Figure, surface free energy (ΔG_S) and free energy of volume (ΔG_V) are represented by solid lines, and their sum by a dashed line. The spontaneous formation of nuclei occurs when the free energy becomes positive at a critical cluster radius, i.e., once a nucleus is large enough, the kinetics favor crystallization as the free energy of the crystal volume overcomes the free energy of the glass-crystal interface and the crystal is the energetically favored state. [1], [30]

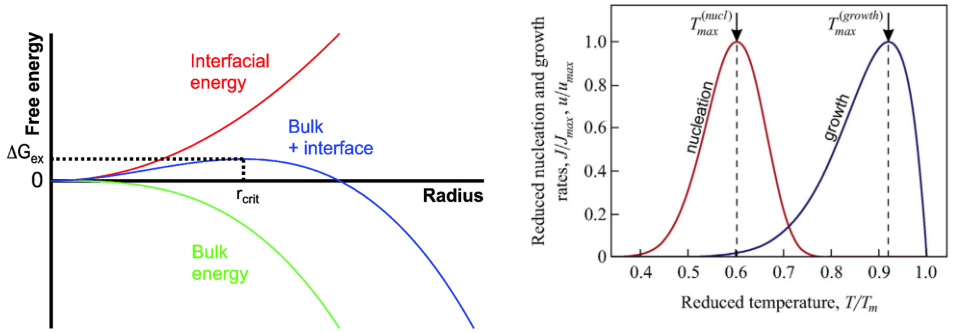

Figure 6. Free energy of a cluster of atoms as a function of cluster radius (a) and a nucleation - growth rates as a function of temperature (b).[31], [32]

- **Crystal Growth:** Following nucleation, the crystalline nuclei develop into crystals during the second stage, known as crystal growth. This two-step process allows for control over crystal dispersion (number density) by adjusting the nucleation time and temperature profile and the resulting crystal sizes by modifying the crystal growth temperature profile.

Figure 6b, shows that the nucleation rate peak occurs even before any crystals are formed, underlining the fact that the crystallization process is a two-step process. As the temperature increases, the nucleation rate decreases, and the crystal growth phase

begins. The actual rates and degree of overlap is very composition dependent. If the crystallization temperature is selected at the intersection of the two rate curves (Figure 6b), the crystallization process can be operated in a single step for simplicity. [1], [28], [30]

As the process involves energy minimization between the free energies of the crystal surface and volume, the crystallization process is location specific. Crystallization can occur in a process known as surface crystallization. Here, the crystals initiate from the air-glass interface and grow inwards, possibly preventing the formation of crystals in the volume of the glass if the growth rate is sufficient. Therefore, the control and understanding of different types of crystallization processes are essential in the synthesis of glass-ceramic materials. [1], [28], [30]

An alternative possibility, not covered in this thesis, to create shaped glass ceramics is the introduction of crystallized particles within the glassy matrix during the glass forming process. The advantage is the control of the nature of the crystalline particles independently of the glass composition. However, the main drawback is the difficulty to obtain homogeneous dispersion of the crystals in the glass matrix and also to avoid any reaction with the glass component. The formation of aggregates, which are detrimental to the transmission properties, should be also limited. [33]

2.2.2 Transparent glass -ceramics

Transparent glass-ceramics are a subclass of glass-ceramic materials that exhibit transparency to light. For transparent glass-ceramics to function effectively, it is essential to achieve bulk crystallization while ensuring, in the same time, that crystalline sizes remain well below the incident wavelength, typically in the order of tens of nanometers at most.[1], [34] As depicted in Figure 7, the transparency of glass-ceramics is determined by two other factors: the size of the crystals and the refractive index mismatch between the glass matrix and the crystals.

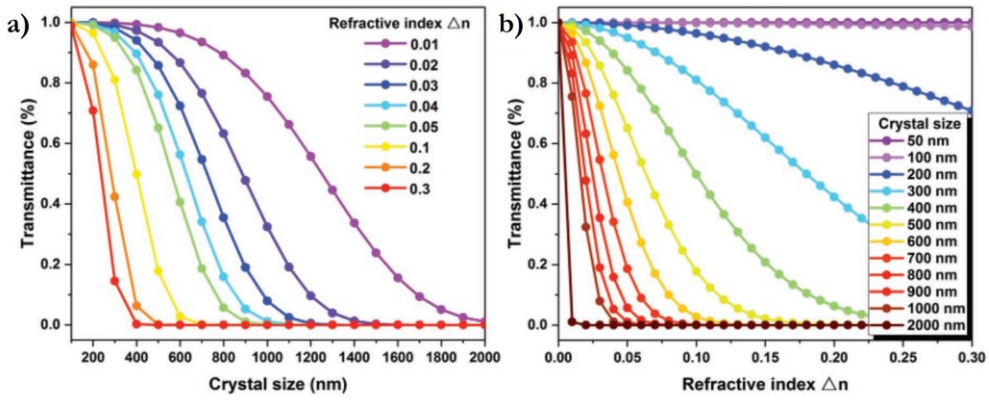

Figure 7. Calculated relationship of transmittance as a function of crystal size (a), and refractive index mismatch (b) for transparent glass ceramics due to Mie scattering.[33]

Mie scattering occurs when the size of the particles or inclusions in a medium are comparable to the wavelength of light passing through it. In the context of transparent glass-ceramics, Mie scattering can lead to a reduction in transmittance when the size of the embedded crystals or the refractive index mismatch between the glass matrix and the crystals is not well controlled, as depicted in Figure 7. [34]. By controlling the nucleation and crystal growth parameters, it is possible to fine-tune the dispersion and size of the crystals in the glass-ceramic. If the refractive index mismatch between the crystals and the glass matrix is small, the transmittance of the material remains high. Conversely, if the refractive index mismatch is large, the crystal size must be minimized to avoid significant degradation of the material's transmittance.[28], [30], [34]

2.2.3 Advantages of glass ceramics

The thermal conductivity of a material can be described as its ability to transfer heat, and in the context of glasses and glass-ceramics, it varies significantly due to their contrasting structures. Glasses, being amorphous, present a disordered atomic structure which in turn induces a low thermal conductivity compared to other materials as seen with crystalline and amorphous silicon dioxide where the thermal conductivity differs by orders of magnitude. The heat transfer primarily occurs through lattice vibrations, phonons, but their movement is impeded by the disordered arrangement, leading to an enhanced phonon scattering. and thus, slower heat propagation and a lower thermal conductivity. This distinctive attribute of

glasses, particularly phosphate glasses, has been applied advantageously in insulation applications and in sectors requiring thermal management.[35] In contrast, glass-ceramics exhibit a significantly higher thermal conductivity than their glass counterparts due to the crystalline regions within the glass matrix which facilitate transfer of heat through the lattice, reducing phonon scattering and thus, augmenting the material's thermal conductivity. Additionally, the thermal conductivity of glass-ceramics can be fine-tuned by controlling the degree of crystallization, allowing the creation of a spectrum of materials with tailored thermal properties. [35], [36]

When we talk about mechanical strength, it usually refers to how well a material can handle pressure or stress without breaking. In the case of glass-ceramics, they are stronger materials than glasses because they have small bits of crystalline material spread throughout the glass matrix. These crystals can prevent the crack propagation, which makes the material tougher and less likely to break. This is a big advantage over glasses, which can break suddenly and completely because cracks cannot be stopped from growing. [28] Another property to consider is hardness, or how well a material can resist to scratch for example. Generally, glass-ceramics are harder than glasses as the crystals are harder than the surrounding glass, so they make the whole material harder overall. This means that glass-ceramics are not just stronger and tougher, but also more resistant to wear and tear compared to glasses. [28]

2.3 Yb^{3+} doped materials

2.3.1 Ytterbium ions

Ytterbium (Yb) is a rare earth element belonging to the lanthanide series. The trivalent ytterbium ion (Yb^{3+}) is particularly advantageous as a lasing element due to its unique energy level structure, which features two primary energy levels (Figure 8), resulting in a reduced susceptibility to concentration quenching and a high quantum efficiency. Yb^{3+} can be efficiently excited using commercial semiconductor lasers at 980 nm, allowing for high-power operation at around 1 μm emission, with low internal losses in the lasing medium, as the nonradiative transitions are confined within the main levels (low quantum defect). Depending on the splitting of the Yb^{3+} energetic levels by the crystal field which depends on the Yb^{3+} environment (coordination number and symmetry), Yb^{3+} doped materials are considered as quasi-

3 level laser (orange arrow), depending on the thermal population of the $^2F_{7/2}$ sublevels (blue arrows), as illustrated in Figure 8. [37]–[40]

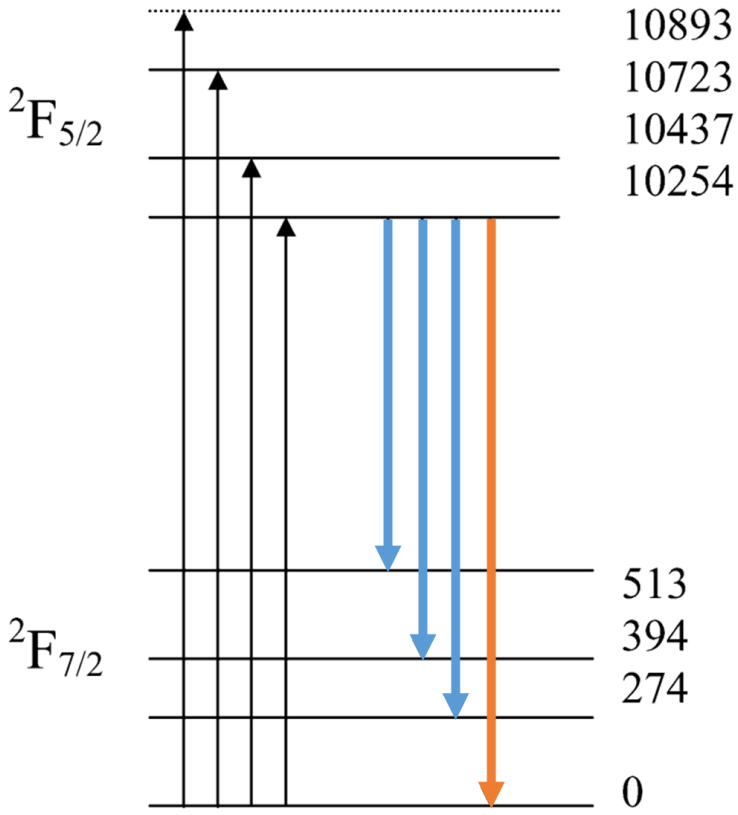

Figure 8. The energy level diagram of trivalent ytterbium ion in a phosphate host, with the most common transitions shown with arrows. The numbers denoting energy in wavenumbers. Modified from [40]

2.3.2 Ytterbium doped glass -based materials

Yb^{3+} -doped glasses offer several advantages over crystals, including their ease of fabrication, excellent optical quality, and the possibility of achieving high doping concentrations. These materials have been widely used in the development of fiber lasers and amplifiers (section 2.4), as well as various solid-state laser systems. Most of the reported work has been done on silicate glasses [41]. Alternative compositions such as phosphates and heavy metal oxide glasses have received minor attention

despite their potential use in ultrashort pulse generation and tunable lasers [42] and in high power and tunable short pulse generation lasers in addition to non-linear laser and amplifier applications [43], [44].

Crystals doped with Yb^{3+} ions have been employed in various laser systems, owing to their high thermal conductivity, excellent mechanical and thermal properties, and the ability to achieve high doping concentrations [6]. As crystals have periodic lattices, the active ions are located in similar environments through the material and thus the emission spectrum is defined with few narrow emissions bands. Some common examples of Yb^{3+}-doped crystals include Yb:YAG, Yb:YLF, and $Yb:YVO_4$. Due to high efficiency, these materials have found applications in high-power lasers, mode-locked lasers, and laser cooling systems.[38] However, a drawback of crystals is their manufacturing as the material should be a single, defect free crystal cut and polished along the crystal planes for optimum performance, leading to high relative cost. Therefore, it is no wonder that Yb^{3+}-doped transparent glass-ceramics have attracted considerable attention as the incorporation of ytterbium ions in the crystalline phase of the glass-ceramic matrix could result in a more uniform distribution of the dopant, thereby reducing concentration quenching effects and improving the overall performance of photonic devices as demonstrated in [28], [30], [34]. For example, Yb^{3+}-doped aluminosilicate oxyfluoride glass-ceramics were obtained via a single step heat treatment [45]: the thermal treatment led to the precipitation of YF_3 nanocrystals. $Yb^{3+}/Er^{3+}/Cr^{3+}$ triply doped glass-ceramic containing Yb^{3+},Er^{3+}:YF_3 and Cr^{3+}:Ga_2O_3 nanocrystals were also investigated due to efficient suppression of adverse energy transfer among active ions due to spatial isolation. [46] Tm^{3+}-Yb^{3+} co-doped oxyfluoride glass-ceramics containing LaF_3 nanocrystals were successfully prepared with an increased quantum efficiency upon a single step thermal treatment with the rare earth elements replacing La in the nanocrystals [47]. Oxyfluoride glass-ceramics showed promising optical applications due to the presence of PbF_2 nanocrystallites in the glass-ceramics after a single-step heat treatment [48] This was followed on by a study PbF_2 single crystals doped with YbF_3 and transparent oxyfluoride glass-ceramics containing nanocrystallites were obtained, highlighting the potential of these materials as good laser media.[49]. One should mention that most of the research on Yb^{3+} containing glass-ceramic has been on co-doped systems.

Surprisingly, research on the development of novel Yb^{3+} doped glass-ceramics has been lacking surprisingly despite the great potential of such materials for photonics

applications clearly showing the importance of the research performed here on the development of new Yb^{3+} doped glass-ceramics (**Publications 1 and 2**).

2.4 Optical fiber

An optical fiber consists of a core, where the light propagates, and a cladding, which confines the light within the core by total internal reflection, as seen in Figure 9. Total internal reflection is achieved only when the core glass has higher refractive index than the cladding for the light to be guided along the fiber.

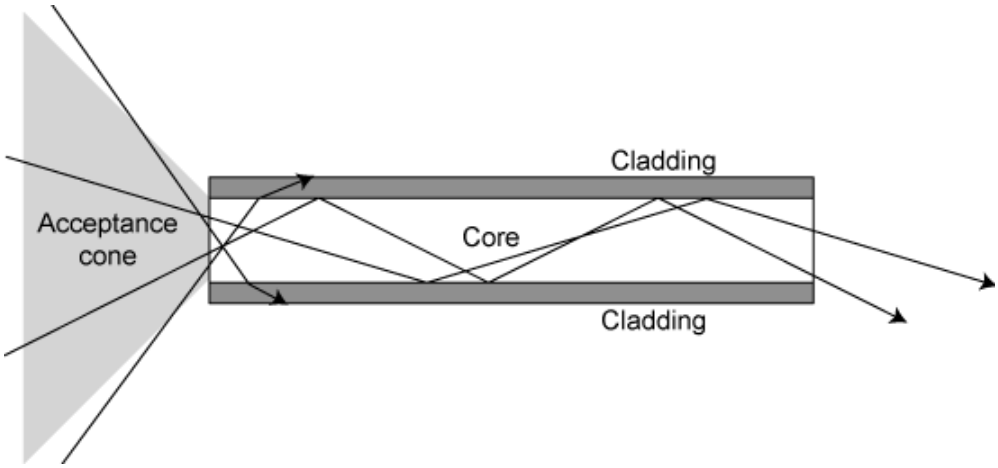

Figure 9. Schematic diagram of the construction of an optical fiber.[50]

2.4.1 Optical fiber fabrication using stack-and-draw technique

To manufacture an optical fiber, a preform, which is a large-scale version of the fiber, must first be created. The preform fabrication process is integral to the optical fiber's quality, and several methods have been developed to prepare preforms with high quality (low number of defects such as bubbles and of impurities). The methods that can be used to manufacture high quality fiber with low losses over hundreds of kilometers, include Chemical Vapor Deposition (CVD), Modified Chemical Vapor Deposition (MCVD), Vapor Axial Deposition (VAD), and Outside Vapor

Deposition (OVD) [51]. Although these industrial methods have proven effective in producing high-quality optical fibers, they are mostly suited for silica-based glasses.[51] Consequently, alternative techniques such as rod-in-tube and stack-and-draw have been developed to meet the requirements of other glass types, such as phosphate glasses, or small-scale experiments without the need for expensive preform fabrication equipment.

- **The rod-in-tube technique** is a relatively simple method of preform fabrication, making it an attractive option for laboratory-scale applications. In this process, a solid rod, which constitutes the core material, is inserted into a hollow tube made of the cladding material, slightly modified in composition to allow for total internal reflection. The assembly is then heated to soften the materials and fuse them together, forming a single, solid preform. The rod-in-tube method offers several advantages over industrial methods, such as lower costs and reduced complexity. However, it may be limited in its ability to produce fibers with complex core structures or precise dopant distributions. Additionally, the process can introduce impurities, inhomogeneities that lead to density fluctuations or defects, especially at the core-cladding interface, which can degrade the fiber's optical properties.[52]

- **The stack-and-draw technique**, also known as the mosaic method, offers an alternative approach to preform fabrication and is a well-established technique for the fabrication of fiber with unconventional geometries (Figure 10). Here, multiple layers of core and cladding material are stacked together in a precise arrangement, forming a preform with a complex structure. The stack is then consolidated by heating it. The temperature should be high enough for the layers to fuse together but low enough to avoid crystallization. Once the preform has cooled, it can be drawn into fiber.[53]

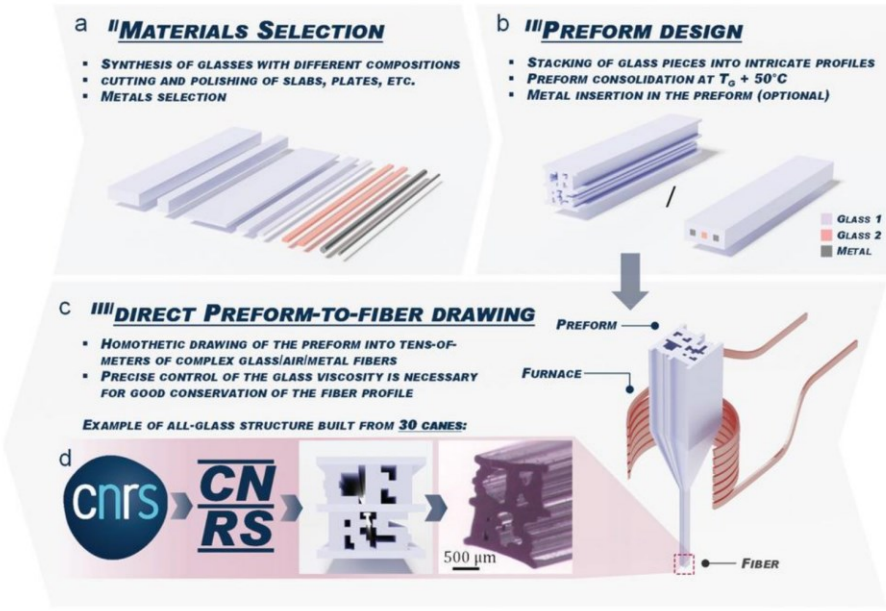

Figure 10. Schematic diagram of the stack-and-draw process[54]

The stack-and-draw technique offers several benefits over the rod-in-tube method, particularly in terms of the versatility of the fiber structures that can be produced. This method allows for the creation of fibers with multiple cores or complex core geometries, which can be tailored to specific applications.[54], [55] Additionally, the stack-and-draw technique provides great macroscale control over dopant concentrations and distribution, enabling the precise tuning of the fiber's optical properties. Finally, the method is highly scalable, enabling the production of long fibers with consistent cross-sectional patterns. [56] However, this method is more labor-intensive and time-consuming than the rod-in-tube technique, as it requires the careful assembly of the multiple layers that make up the preform.

One of the critical factors in the stack and draw method is the choice of glass material and understanding its behavior during the fabrication process. The material's thermomechanical properties, such as viscosity, play a significant role in determining the success of the process. In the case of multimaterial fibers, which makes use of doped and undoped glasses together, the thermal compatibility (similar thermal properties such as glass transition and crystallization temperatures and similar viscosity and thermal expansion coefficient) of the components in the stack is essential. This compatibility ensures that the fiber maintains its structural integrity

and desired optical and mechanical properties during the drawing process Additionally, there are also challenges associated with the stack and draw method. The stacking process can be labor-intensive and time-consuming, particularly when constructing complex patterns.[54]

After the preform fabrication, the next step is to draw the preform into an optical fiber. The drawing process is critical in determining the fiber's final dimensions, optical properties, and mechanical strength. A typical drawing tower, presented in Figure 11, consists of a furnace, where the preform is heated to its softening point, a drawing mechanism that pulls the softened preform into a fiber, and a diameter monitoring system that ensures the consistent fiber dimensions along its length. In addition, a polymer coater can be used, although the coater is often omitted in research towers.[57]

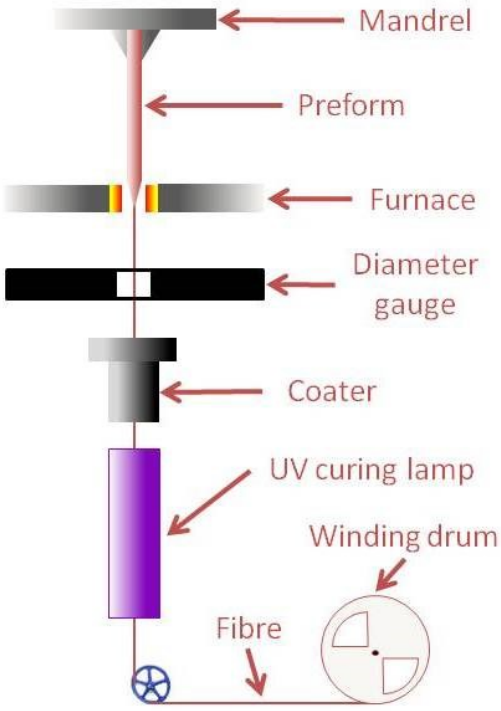

Figure 11. A schematic diagram of a fiber optic drawing tower.[58]

2.4.2 Yb^{3+} doped fiber

Ytterbium-doped fiber lasers have emerged as one of the most promising laser technologies due to their high output power, excellent beam quality, and tunable wavelength capabilities. [37]

2.4.2.1 Latest Yb^{3+} doped fiber development

The current research for the past 10 years on Yb^{3+}-doped optical fibers can be roughly divided into four categories: **1 –** high average power lasers and related efforts in attempts to achieve high laser power while minimizing negative effects such as photodarkening and modal instabilities; **2 –** next generation of Yb^{3+}-based femtosecond lasers; **3 –** various codoping schemes for photon upconversion or MIR emission and **4 –** optical refrigeration. Here are given few examples of the latest development in these 4 fields:

1. A theoretical study of mode instabilities in Yb^{3+}-doped fiber explores the impact of various fiber and system parameters, multi-wavelength pumping configurations, pump wavelength shifting in tandem pumping technique, and amplitude modulation. These mitigation methods present a way to surpass mode instability limitations for achieving over 10-kW diode-pumped fiber laser output.[59] Effort has been focused on limiting the degradation of the fiber during lasing (see next section on photodarkening)
2. An environmentally stable source based on cascaded Mamyshev regeneration is offering at least an order of magnitude higher peak power than previous lasers with similar fiber mode area. Numerical simulations suggest that peak powers nearing 10 MW are attainable from an ordinary single-mode fiber, after external linear compression and 1 MW pulses are demonstrated.[60]
3. A transparent Yb^{3+}-Er^{3+} codoped glass-ceramic fiber, obtained through a melt-quenching method, displayed significantly enhanced upconversion luminescence following heat treatment due to the precipitation of CaF2 nanocrystals.[61]
4. Laser cooling has been reported in a Yb^{3+} -doped silica optical fiber. Using a custom slow-light fiber Bragg grating sensor, temperature reductions up to -50mK were measured at an absorbed pump power of 0.33 W/m, aligning with established models, underscoring the fiber's potential for application in radiation-balanced fiber lasers.[62]

In the context of this thesis, the research has focused on the aspects 1 and 3, in developing new transparent Yb^{3+} doped glasses and glass-ceramics (**Publications 1-**

2) which could be drawn into fibers (**Publication 4**) including the investigation of their response to radiation treatment (**Publication 3**).

2.4.2.2 Photodarkening process

The photodarkening process can occurs when the high intensity light causes damage to the glass structure. The damage results in an increased optical absorption that reduces the fiber transmittance and increases the thermal losses. Photodarkening can be attributed to various mechanisms, such as color center formation, ionization-induced defects, and the generation of various hole/electron centers under high intensity light. This glass-light interaction leads to electrons moving around and forming areas that have a deficit (holes) or excess electrons and these areas can be optically active, i.e., absorb light in specific spectral regions.[63]–[66]

Two primary mechanisms have been proposed to explain the formation of color centers in ytterbium-doped silica glasses, shown in Figure 12. The first mechanism involves the excitation of Yb^{3+} ions to a higher-energy state, followed by energy transfer to the surrounding glass matrix, which creates a defect. [67]

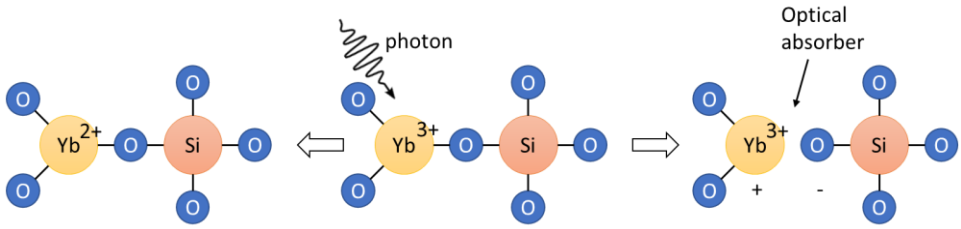

Figure 12. Highly simplified schematic diagram showing the potential primary mechanisms of color center formation.

An alternative mechanism was suggested by Rybaltovsky et al: the pump light leads to the ionization of Yb^{3+} ions under high-intensity light, resulting in the formation of Yb^{2+} ions and the generation of optically active defects within the glass matrix. [68] These color centers are a general term for atomic-scale defects that arise from the presence of unpaired electrons or ions within the glass matrix, causing characteristic absorption bands in the optical spectra.

Photo-darkening in Yb^{3+} doped glasses is also influenced by various factors such as the glass composition, doping concentration, and the presence of impurities. For instance, glasses with high concentration of ytterbium ions are more prone to photo-darkening due to the increased probability of energy transfer and ionization processes.[69] Additionally, impurities within the glass matrix, such as transition metal ions, can act as trapping centers for photo-generated carriers, further enhancing the photo-darkening effect.[70] To address these challenges, several mitigation strategies have been proposed, such as modifying the glass composition, optimizing the doping concentration, and incorporating co-dopants to reduce the formation of color centers.[69], [71]

It is thus crucial to understand similarities and differences in glass-light interaction between various Yb^{3+} doped glass types. Here the study on glass-radiation interaction was focused on phosphate, borosilicate, and heavy metal oxide glasses, such as germanate and tellurite glasses (**Publication 3**).

- **Phosphate glasses** were reported to exhibit radiation-induced coloration, or photodarkening, because of the formation of radiation-induced defects, such as electron and hole centers that are usually formed at the P-O bond as ionizing radiation ejects electrons to create the intrinsic hole/electron defects in phosphate glasses.[72]

- **Borosilicate glasses** are known for their radiation resistance and are commonly used in nuclear waste immobilization applications.[73] However, they are not immune to radiation effects neither to formation of point defects. The exposure to ionizing radiation can lead to the creation of several types of defects within these glasses, which can subsequently alter their optical, mechanical, and structural properties. The main radiation-induced defects in borosilicate glasses include color centers, electron/hole centers, and structural changes. Electron-hole centers, also known as paramagnetic defects, are another class of radiation-induced defects in borosilicate glasses. They are formed when an electron is trapped in an anion vacancy, or a hole is trapped in a cation vacancy.[65]

- **Germanate and tellurite glasses** can exhibit radiation-induced defects and changes in the glass structure. For instance, radiation-induced color centers, such as self-trapped holes, can lead to photodarkening process in germanate glasses. Tellurite glasses, on the other hand, can exhibit radiation-induced structural changes, such as the formation of non-bridging oxygen atoms and the alteration

of tellurium coordination. The radiation sensitivity of these glasses depends on factors such as the glass composition, the presence of dopants, and the radiation conditions.[74]

For more information on photo-response of glasses, the reader is referred to [74].

2.4.3 Biophotonic fibers and applications

Another application of optical fibers is in the field of biomedical diagnostics. These fibers can be used to transmit light into biological tissues, collect and analyze the resulting signals, and relay the information back to an external detector. This approach enables minimally invasive and real-time monitoring of various physiological parameters, such as oxygen saturation, blood flow, and tissue metabolism.[26] Moreover, the flexibility and small size of the fibers allow for easy integration into endoscopic devices, which further expands their potential applications to direct imaging.[55] In addition to diagnostics and imaging, biophotonic optical fibers have shown great promise in the field of therapeutic applications. One notable example is photodynamic therapy (PDT), which involves the use of light to activate a photosensitizer, which could be used for the generation of reactive oxygen species and subsequent cell death. By coupling the light from a laser source to a biophotonic optical fiber, it is possible to deliver the required light dose to the target tissue with high spatial precision and minimal damage to surrounding healthy tissues. This approach has been successfully employed in the treatment of various cancers, including head and neck, lung, and gastrointestinal malignancies.[75]

In recent years, there has been a growing interest in the development of multifunctional optical fibers, which combine multiple functionalities within a single fiber structure. These fibers can be designed to simultaneously perform diagnostic, imaging, and therapeutic tasks, thereby enabling a more streamlined and efficient approach to patient care. For instance, researchers have developed fibers capable of both sensing and delivering light for PDT and to simultaneously deliver liquids via the built-in capillary structure, allowing for real-time monitoring of the treatment progress and facilitating precise and targeted therapy.[76]

Biophotonic fibers are defined, in this thesis, as a bioactive glass which is also a laser glass. Here a borosilicate glass was doped with Yb^{3+} (**Publication 4**). This glass was

previously reported to be bioactive in [77]. Our goal is to demonstrate that it is possible to track overtime and in-situ the fiber reaction with the body from the changes in the Yb^{3+} spectroscopic properties. Two types of fibers geometry will be tested.

3 EXPERIMENTAL METHODS

3.1 Glass synthesis

3.1.1 Bulk melting

This study explores the preparation and characterization of various Yb^{3+} doped glasses with different compositions and dopant concentrations. The investigated glasses include phosphate, tellurite, borosilicate, germanate, and fluoride-containing sodium phosphate glasses, the composition of which is given in Table 1. The melt-quench method is employed to process these glasses.

Table 1. Composition of the investigated glasses

Glass code	x	Composition (mol-%)
Ca-phosphate	-	98.75 (50 P_2O_5 - 40 CaO - 10 Na_2O) – 1.25 Yb_2O_3
Sr-phosphate	-	(100-x) (50 P_2O_5 - 40 SrO - 10 Na_2O) - x Yb_2O_3
F (x)	0 to 10	(98.75-x)(90 $NaPO_3$ – 10 Na_2O – x NaF) – 1.25 Yb_2O_3
Al (x)	0 to 3.0	(98.75-x)(90 $NaPO_3$ – 10 Na_2O) – x Al_2O_3 – 1.25 Yb_2O_3
Ti (x)	0 to 3.0	(98.75-x)(90 $NaPO_3$ – 10 Na_2O) – x TiO_2 – 1.25 Yb_2O_3
Zn (x)	0 to 3.0	(98.75-x)(90 $NaPO_3$ – 10 Na_2O) – x ZnO – 1.25 Yb_2O_3
Borosilicate (x)	0 to 1.25	(100-x) (26.93 SiO_2 - 26.93 B_2O_3 - 22.66 Na_2O - 1.72 P_2O_5 - 21.76 CaO) - x Yb_2O_3
Germanate	-	98.75 (64.6 GeO_2 - 10 Ga_2O_3 - 11.4 BaO - 5 TiO_2 - 9 Na_2O) – 1.25 Yb_2O_3
Tellurite	-	98.75 (80 TeO_2 - 10 ZnO - 10 Na_2O) – 1.25 Yb_2O_3

The raw materials used to synthesize the glasses are presented in Table 2. All chemicals were anhydrous unless otherwise mentioned.

Table 2. Raw materials used in glass synthesis, purity, and supplier.

Raw Material	**Purity**	**Provider(s)**
Al_2O_3	≥99%	Sigma
BaO	≥99.99%	Sigma

B_2O_3	99.9%	Merck
$CaCO_3$*	99.9% (Sigma-Aldrich), ≥99.0% (Alfa Aesar)	Sigma-Aldrich, Alfa Aesar
$CaHPO_4 \cdot 2H_2O$	Puriss.	Sigma
Ga_2O_3	≥99.99%	Sigma
GeO_2	≥99.99%	Sigma
H_3BO_3	≥99.5%	Sigma
Na_2CO_3	100.05% dry basis (Alfa Aesar), ≥99.5% (Sigma), 99.8% (Sigma-Aldrich)	Alfa Aesar, Sigma, Sigma-Aldrich
Na_3PO_4	96%	Sigma-Aldrich
NaF	99.99%	Sigma-Aldrich
$NaPO_3$	Tech.	Sigma, Alfa Aesar
$(NH_4)_2HPO_4$*	≥99.0%	Sigma
SiO_2	99.5% (Alfa Aesar), ≥99.99% (Umicore)	Alfa Aesar, Umicore
$SrCO_3$*	≥98%	Sigma
TeO_2	≥99%	Sigma
TiO_2	≥99.8%	Sigma
Yb_2O_3	99.9% (ABCR), ≥99.9% (Sigma)	ABCR, Sigma
ZnO	≥99.99%	Sigma

*$Sr(PO_3)_2$ and $Ca(PO_3)_2$ were first synthesized in according to procedure detailed in [78] from $(NH_4)_2HPO_4$ and $SrCO_3$ or $CaCO_3$, respectively.

The glasses were melted in either quartz or platinum crucibles, depending on the glass type, and subjected to specific melting temperatures: 1125 °C for phosphate glasses, 1275 °C for borosilicate glass, 1600 °C for germanate glass, and 850 °C for tellurite glass. After melting, the glasses were quenched and annealed at temperatures 40 °C below their respective glass transition temperatures (T_g) for 6 hours.

3.1.2 Glass ceramics preparation

Oxyfluorophosphate glass-ceramics were prepared using a two-step treatment. After annealing, the glasses were heat treated at their respective (T_g+20 °C) for hours to create the nuclei and then at higher temperature to grow them into crystals

3.1.3 Preform fabrication and drawing

Round and square preforms were prepared from the borosilicate glasses with x=0 (cladding) and x=1.00 (core) to offer a refractive index contrast and probing functionality.

To create the preforms with round cross-sections, the undoped glass (intended as the cladding) was first poured into a preheated graphite mold. This was followed by plunging a graphite rod into the melted glass (Figure 13a). This rod was rapidly extracted, leaving a void which was then filled with the Yb^{3+} doped core glass. The complete preform, still encased in the graphite mold, was annealed. After cooling to room temperature, the preform surface was polished optically using abrasive papers to remove any graphite prior to the drawing process. This method allowed the preparation of cylindrical glass preforms with a diameter of 8 mm and a length of approximately 7 cm.

Creating the rectangular preforms leveraged the stack-and-draw method, as detailed in Figure 13b. Initially, bulk glass pieces were cut into rectangular blocks and optically polished on the joint sides (with average dimensions: length 6 cm, width: 1 cm, thickness: 0.5 cm). A three-part assembly was heated to 575 °C, which corresponds to T_g+60 °C for one hour under a consistent pressure of around 100 g cm^{-2}. This stacking step was repeated to finalize the desired geometry. Prior to the drawing process, all four sides were polished to an optical finish.

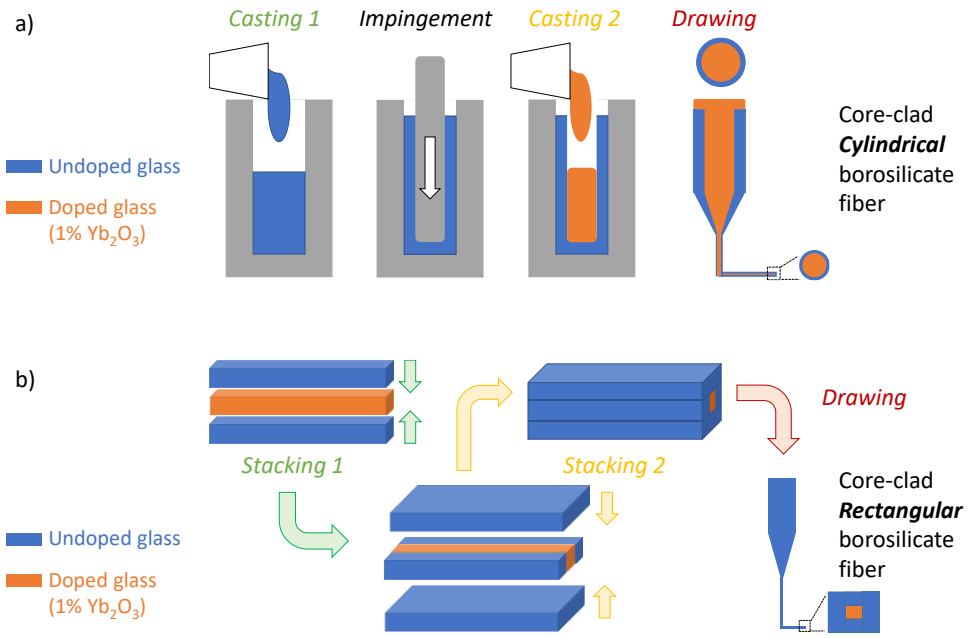

Figure 13. Schematic diagram of the manufacturing process for the preforms using the impingement method (a) and stack-and-draw (b).

The preform was then drawn as detailed in section 2.4.1. Special care was taken to avoid twisting of the fiber during drawing as the fiber is not round.

3.2 Thermal, physical, morphological, and mechanical properties measurement

3.2.1 Thermal properties

Netzsch DTA 404 PC with Pt-Ir crucibles and JUPITER F1 with Pt crucibles were used to measure the thermal properties of these glasses and glass-ceramics. Figure 14 Figure 14. shows a thermogram of typical glass.

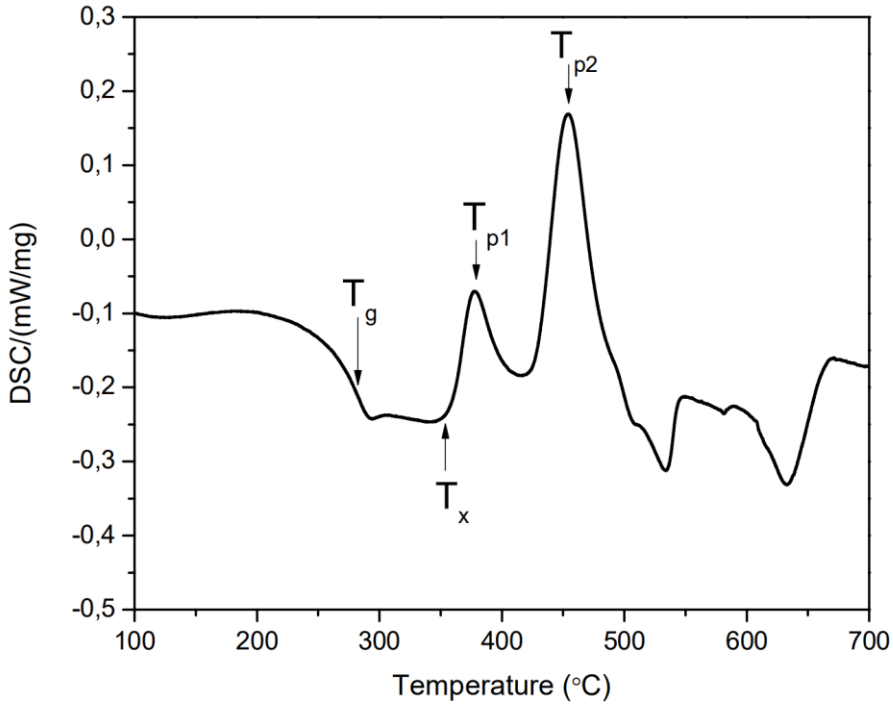

Figure 14. A DSC curve of a glass, showing the locations of the different critical temperatures, including two different crystallization peaks.[79]

The glass transition temperature (T_g) was given by the minimum of the first derivative of the thermogram, the onset of crystallization (T_x) by the tangent intersection at the exothermic crystallization peak and the peak crystallization temperature (T_p) as the maximum of the first exothermic peak. The difference between the glass transition temperature and the onset of crystallization is called delta-T ($\Delta T = T_x - T_g$). This parameter is important when evaluating the thermal stability of glass. A glass with a value over 90 °C is generally considered as good glass former and no crystallization is expected to occur during the drawing process. The temperatures are given at ± 3°C.

3.2.2 Density Measurement

The density of the glasses was determined using the Archimedes' method, OHAUS Adventurer and Precisa XT220A laboratory scales with their density measurement kits were used here. Immersion fluid was absolute ethanol or diethyl phthalate, respectively. Accuracy of the measurement is ± 0.02 g cm^{-3}.

3.2.3 Mechanical properties

Microhardness was measured using Leica VMHT with a Knoop diamond tip and a 9.81N (10 g) force on polished samples. Measurement was repeated 12 times at different areas of the sample. Microhardness is given at ±10 %.

3.2.4 Surface Roughness

Wyko NT1100 was used to measurement the roughness parameters (R_a the arithmetic mean deviation and R_q the quadratic mean roughness). Accuracy was ±10% when considering localized variations of a single surface.

3.2.5 X-ray Diffraction (XRD) Pattern

Panalytical EMPYREAN and X'Pert Pro with copper or cobalt K_α radiation were used in this study to investigate the crystallinity of these materials. The samples were crushed into powder by hand, placed on Si or Al sample holders and their X-ray diffraction patterns were measured from 8 to 80° 2θ angle.

3.3 Composition analysis

Zeiss Leo 1530 Gemini, Crossbeam 540 and TESCAN Vega II SBH electron microscopes were used to image the sample and analyze their composition. X-MaxN 80 by Oxford Instruments was the used for elemental analysis by energy dispersive spectroscopy. The compositions are given at ±1.0 mol%.

3.4 Optical and Spectroscopic properties

3.4.1 Refractive Index

Refractometer by ATAGO with Na D-line (589 nm) light was used for refractive index determination. Accuracy was ±0.001.

3.4.2 Transmittance properties

Cary 5000 or a Shimadzu UV-3600 Plus was used to measure the UV-Vis-NIR absorption spectrum of the bulk samples.

The fiber losses were measured using the cutback method with an accuracy of ±5%. The method involves two steps: first, measuring the optical power transmitted through a known length of the fiber, and second, cutting the fiber to a shorter length and measuring the transmitted power again. The difference in optical power between the two measurements is used to calculate the fiber attenuation coefficient over the cut piece of fiber. [80] Loss was measured using a fiber fed DH-2000-BAL light source and a AvaSpec-ULS4096CL-EVO spectrometer.

3.4.3 Spectroscopic Properties

The emission spectra were measured s using a FLS1000, an iHR320 and a Fluorolog 3 spectrometer with a Xe lamp with the latter using a separate LN_2 cooled DSS-IGA020L InGaAs NIR detector and using a Spectro 320-131 Vis-NIR fed with a 976 nm pigtailed laser diode. The microscopic emission spectra mapping of small samples such as optical fibers, were measured using the confocal microscope system built around LabRAM HR with an external 975 nm laser diode excitation. Samples were either polished bulk samples or finely ground powder held in place by a microscope slide.

3.5 Structural properties

3.5.1 Fourier Transform Infrared Spectroscopy

PerkinElmer Spectrum One and Bruker Equinox 55 were used for the FTIR measurements. Spectrum One was used in ATR mode for the analysis of the structural bands and Bruker Equinox 55 in transmission mode for the analysis of the water absorption.

3.5.2 Raman Spectroscopy

The Raman spectra were measured with Renishaw InVia Qontor and LabRAM HR systems, using diode lasers at 405 and 532 nm for excitation. 1200 and 1800 lines/mm gratings were used as the dispersing elements.

4 RESULTS AND DISCUSSION

New Yb^{3+} doped glasses were developed in this study and their response to thermal and radiation treatment was investigated as well as their response in aqueous medium when drawn into fibers.

4.1 Stability of Yb^{3+} doped glasses under thermal treatment

Glasses in the (98.75-x)(90 $NaPO_3$ – 10 Na_2O – x NaF) – 1.25 Yb_2O_3 system (mol%) with x ranging from 0 to 10 were investigated to prepare transparent glass-ceramics with improved spectroscopic properties.

4.1.1 Thermal treatment to prepare transparent glass-ceramics

The glass-ceramics were obtained using a two-step thermal treatment, with the first step performed at T_g + 20 °C for 17 h. The second step was done at T_p -40 °C for 30 and 60 minutes. The treatments resulted in opaque glasses, clear sign of crystallization. The SEM images (Figure 15Figure 15.) showed needle-like crystals growing from the glass surface.

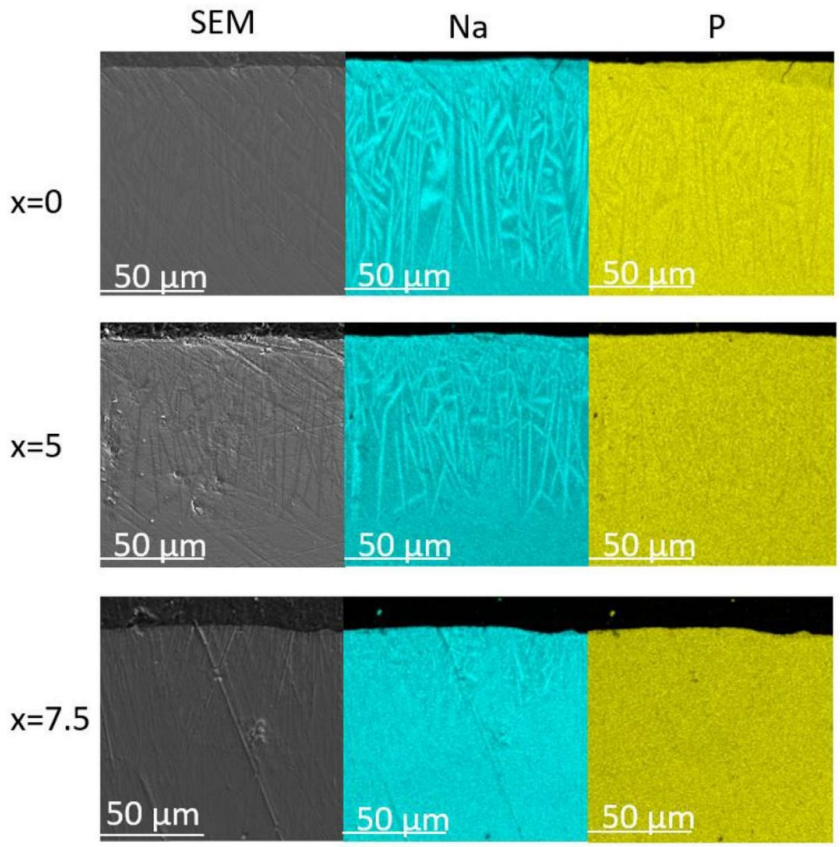

Figure 15. SEM images and elemental mapping taken from the cross-section of the heat-treated glasses

It was found that the thickness of the crystallized layer decreased as x increased, suggesting that the replacement of Na_2O by NaF reduced the crystallization tendency of the glasses. A correlation was found between crystallization tendency and network connectivity. Indeed, an increase in x (NaF at the expense of Na_2O) resulted in a decreased T_g indicating a weaker ionic cross-linking between the modifier cations and non-bridging oxygen. Upon increasing the NaF content, an increase in Q^2 units is seen, counterbalanced by a reduction of Q^1 units (IR and Raman spectra can be found in **Publication 1**).

Various crystalline phases were detected via XRD analysis, including $NaPO_3$, $Na_5P_3O_{10}$, and $NaYbP_2O_7$. With an increase in x, the $NaPO_3$ phase was found to grow at the expense of $Na_5P_3O_{10}$, and a small amount of $Na_4P_4O_{12}(H_2O)$ was

suspected to partially transform into $NaH_2(PO_3)_4$. Further investigation using SEM showed that surface crystallization dominated. However, bulk crystallization was noticed only in the glass with x = 0. The other glasses mainly exhibited surface crystallization. The precipitation of the crystals led to noticeable changes in shape of the emission spectra of the thermally treated glasses with the shoulder at ~1 μm becoming more pronounced relative to the band at 975 nm. Although the emission intensity decreases following heat treatment presumably due to a reduction in Yb–Yb distance, the bandwidth of the emission band increased. It is pertinent to mention that the fully crystallized materials emission spectra match well with the Yb^{3+} emission in $NaYbP_2O_7$ crystals. [81]

As the glass with x=0 is the only glass exhibiting volume crystallization upon thermal treatment, different heat treatments were performed to prepare transparent glass-ceramic (Table 3.).

Table 3. Different heat treatments used to heat treat the glass with x=0.

HT	Nucleation phase	Growth phase
A	T_g + 20°C for 17h	T_p - 40°C for 30min
B	T_g + 20°C for 17h	T_p for 2h
C	T_g + 20°C for 17h	T_p - 40°C for 1h
D	T_g + 20°C for 66h	T_p - 40°C for 30min

As shown in Figure 16 the heat-treatment can lead to precipitation of crystals in the glass volume. The effect is most evident in HT-D, where small XRD peaks are seen at the locations indicated by the black lines, demonstrating the presence of crystals in the glass, while retaining transparency (Figure 16).

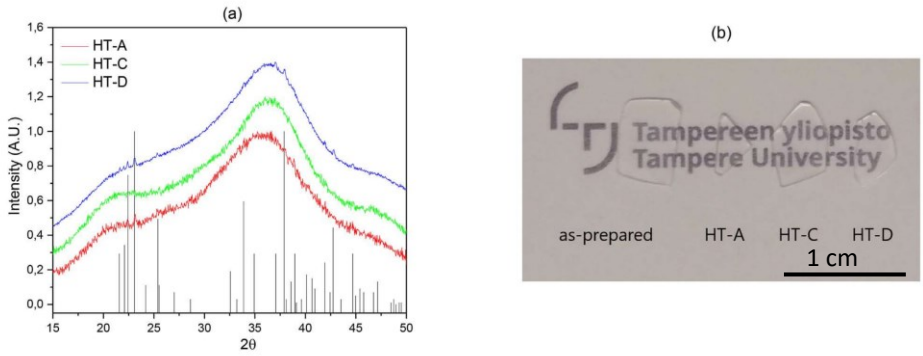

Figure 16. XRD patterns of the glass ceramics after the heat treatments with reference peak locations and intensities of all the crystals observed to grow in the glass after HT-B (a) and picture of the glass with x=0 prior to and after heat treatment (b)

Using SEM, the crystals were found in the volume of the glass confirming that transparent glass-ceramic can be obtained from the glass with x = 0 when using proper parameters (temperature and duration) for the thermal treatment.

However, the glass is hygroscopic which was evidenced from the IR spectrum of the glass. Indeed, the spectrum exhibits an absorption band in the 2250 – 4000 cm^{-1} range with high intensity. This band can be correlated to both weakly associated, or "free" OH groups, and more strongly associated OH groups (absorption spectra published in **Publication 1**). The hygroscopic nature is anticipated based on the composition of the glasses, where high levels of P_2O_5 and Na_2O render the glass more unstable in atmospheric conditions. Fluorine is conventionally used as a drying agent to displace bound OH^- groups within the glass network. Hence, the OH content of the glass inversely correlates with the fluorine content. With an increased proportion of fluorine in the composition (indicated by a higher value of x), a decrease in the intensity of the absorption bands linked to the OH groups was observed confirming the displacement of OH^- groups by fluorine. As a consequence, the progressive replacement of Na_2O by NaF was found to enhance the area of the emission band due to the change in the network connectivity and the reduction in the number of OH^- groups, the latter being recognized quenchers of Yb^{3+} ions.[82] Notably, these glasses exhibit Yb^{3+} $^2F_{5/2}$ level lifetime values which are comparable with those reported for phosphate glasses, but substantially exceeds those found in silicate and tellurite glasses.

4.1.2 Changes in the glass composition to improve resistance against water absorption over time without impacting the nucleation and growth mechanism

In order to improve the chemical stability of the glass with x=0, glasses with the composition (98.75-x) [90 $NaPO_3$-10 Na_2O] – x (Al_2O_3, TiO_2, or ZnO) – 1.25 Yb_2O_3 (in mol-%), with x varying from 0 to 3 (referred to as Al(x), Ti(x), and Zn(x) respectively) were investigated.

The IR spectra of these glasses were recorded post-quenching and after a period of five months. The addition of Al_2O_3, TiO_2, or ZnO resulted in a reduction in the OH band intensity, suggesting a decrease in OH content which is, however, independent of x as seen in Figure 17.

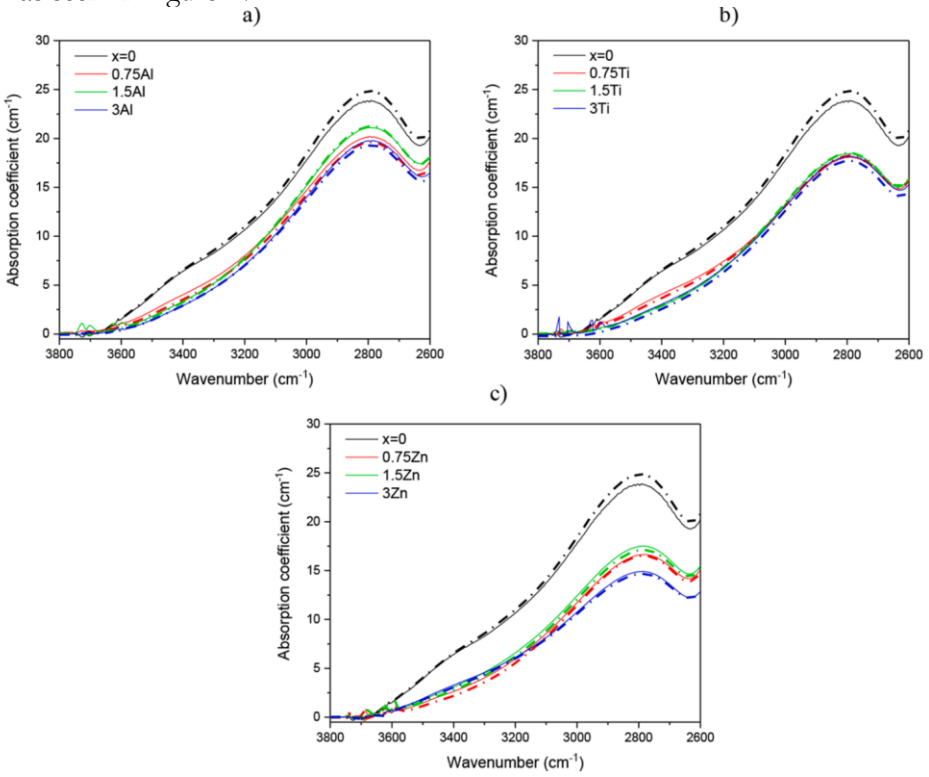

Figure 17. IR absorption spectra of the Al (a), Ti(b), and Zn(c) glasses measured after melting (solid line) and after 5 months (dashed thick line).

The IR spectra were also recorded five months post-synthesis. Minimal changes in the OH band intensity in the Al, Ti, and Zn glasses were seen, while the glass with x = 0 demonstrated a slight increase in OH band intensity, indicative of water absorption over time. Consequently, the Al, Ti, and Zn-doped glasses seem more resilient against water absorption compared to the glass with x = 0, possibly due to their enhanced network (in the case of Al and Ti glasses) or elongated phosphate chains in the case of Zn. Indeed, while the Zn (x) variants demonstrated no significant alteration in thermal attributes, the integration of Al_2O_3 and TiO_2 in Al (x) and Ti (x) respectively resulted in an increase in the glass transition temperature (T_g), the crystallization onset temperature (T_x), and the first crystallization peak temperature (T_p). The ΔT reveals a notable enhancement in the glass's resistance to crystallization when Al_2O_3 or TiO_2 is incorporated, suggesting a strengthening of the phosphate network. This contrasts with the Zn(x) variants, which exhibit ΔT values below 90 ◦C, suggesting their inferior resistance to crystallization. These changes in the thermal properties can be related to the structure of the glasses which was investigated using FTIR (Figure 18).

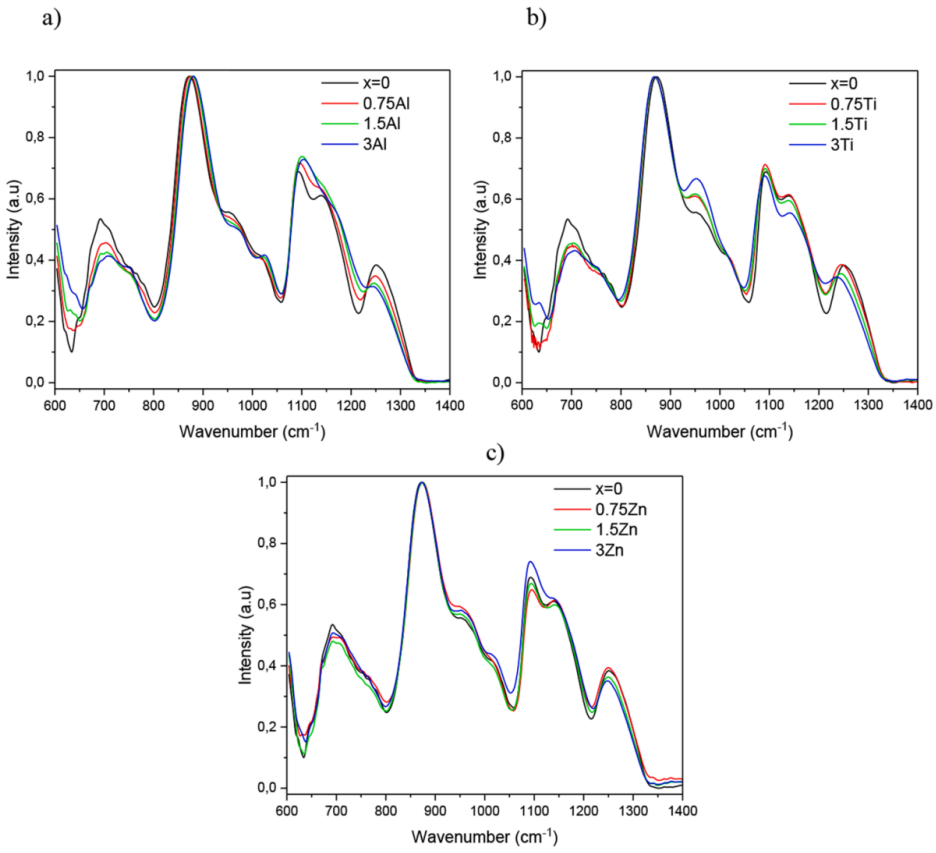

Figure 18. FTIR spectra of the sodium phosphate glasses. Glass series Al (x), Ti (x), and Zn (x) shown subfigures a, b, and c, respectively.

The incorporation of Al_2O_3, ZnO, and TiO_2 leads to a progressive increase in the number of Q^1 units at the cost of Q^2 units. Al ions embed themselves into the network, transitioning non-bridging oxygens into bridging oxygens. This process strengthens the network, enhances network connectivity, and manifests as a shift in the main band at 880 cm^{-1} to longer wavenumbers. The Al (x), together with Ti (x), glasses contain bands attributable to various stretching P-O-(Al/Ti) bands between 600-700 cm^{-1}. The formation of P-O-Ti bonds is confirmed by the diminished IR band at 1090 cm^{-1} and the increase in intensity of the shoulder at 1010 cm^{-1}. As Ti, due to its large charge and small ionic radius, positions itself between the phosphate rings and chains, Ti-O-P cross-linking occurs between phosphate tetrahedra and Ti^{4+} ions, consequently shrinking the size of the rings. This interaction also leads to a

slight shift in the main band position with an increasing Ti concentration. The development of 3D network structures by P-O-Ti linkages, as observed in the spectra, is confirmed by an increase in the glass transition temperature (T_g). In contrast, Zn operates as a modifier in these glasses, causing a depolymerization of the phosphate network, i.e., reduction in network cross-linking or lessening of the connections between linear phosphate chains, as the ZnO concentration increases.

The glasses were heat treated as performed for the glass with x=0. The incorporation of Al_2O_3, TiO_2, and ZnO into the phosphate network altered the crystallization process: it promoted the precipitation of the $Na_5P_3O_{10}$ crystalline phase at the expense of $NaYb(P_2O_7)$ and $NaPO_3$ phases and more importantly the surface crystallization at the expense of bulk crystallization. The addition Al_2O_3, TiO_2, and ZnO increased the thickness of the crystallized surface layer, demonstrating that the newly developed glasses have a higher propensity for crystallization than the glass with x=0. The crystallization behavior is closely related to the rigidity of the glass network, which in turn is influenced by the compositional additives. When Zn is added, the glass network permits a higher cation migration, leading to less precipitation of $NaYbP_2O_7$ crystalline grains. When Al and Ti are added, the glass network remains relatively rigid, limiting Yb^{3+} migration and thus favoring the growth of $NaYbP_2O_7$ particles.

4.1.3 Conclusions

Here, new Yb-doped oxyfluorophosphate glasses and glass-ceramics were prepared and characterized. Transparent glass-ceramic could be obtained by heat treating the F free glass which was found to increase the bandwidth of the Yb^{3+} emission band. However, this glass was found to be hygroscopic, hence limiting its use. Therefore, aluminum, titanium, and zinc oxides were added in the glass to improve its resistance to water. The glasses' resistance against water was enhanced by adding oxides, illustrating the importance of compositional adjustment in the modification of glasses' properties. However, the changes in the glass composition led to changes in the nucleation and growth mechanism: the incorporation of Al_2O_3 and TiO_2 not only resulted in an increased resistance to crystallization but also prevented bulk crystallization, demonstrating the role of Al_2O_3 and TiO_2 as network strengtheners. On the contrary, the Zn(x) variants displayed inferior resistance to crystallization, indicating that Zn may not play a significant role as a network strengthener.

In conclusion, the comprehensive study of Yb^{3+} -doped oxyfluorophosphate glass-ceramics has opened new pathways for improving the spectroscopic properties of glass-based materials. The findings demonstrate that fine-tuning the composition can be used to enhance water resistance. However, changing the glass composition may influence the crystallization process.

4.2 Stability of Yb^{3+} glasses under radiation treatment

Understanding the stability of Yb^{3+} -doped glasses under radiation treatment is a critical aspect in the development and application of these materials. It is noteworthy that a significant proportion of studies related to the photo-response of Yb^{3+} -doped glasses have been concentrated predominantly on silica glass. However, alternative glass systems also present great potential as hosts for Yb^{3+} ions. This section aims to explore these alternative glass systems, especially focusing on the impacts of radiation treatment on their optical and spectroscopic properties.

4.2.1 Selected Yb^{3+}-doped glasses

Silicate glasses, including borosilicate glasses, are the most common glass types, finding use in nearly all applications so their inclusion in a comparative study is well justified. Among the alternative glass materials, Yb^{3+} -doped phosphate glasses have shown promising characteristics (broad absorption and emission bands coupled with a high absorption/emission cross-section), rendering them as potential materials for generating ultrashort pulses and tunable laser sources. Similar applications and features are exhibited by the Yb^{3+} -doped germanate and tellurite glasses, making them suitable candidates for high peak-power and high-average-power lasers and short pulse generation tunable lasers. These glasses exhibit a wider transmission range than silica and silicate glasses and have lower phonon energies, ideal for non-linear laser and amplifier applications. [74]

The present study on glass response to radiation treatment involves two different phosphates (Sr and Ca glasses), borosilicate, germanate (Ge), and tellurite(Te) glasses. Composition of the glasses can be found in Table 1. The complete analysis of the thermal, optical, structural, and spectroscopic properties of these glasses can be found in **Publication 3**.

4.2.2 Response of Yb^{3+} doped glasses to radiation treatments using electrons and protons.

The glasses were irradiated with electrons and protons in collaboration with Dr. Laura Mihai from National Institute for Laser, Plasma and Radiation Physics, Romania. The particle energies, doses, calculated penetration depths, and irradiation times for each radiation type are provided in Table 4.

Table 4. Doses, penetration depths and irradiation times used for the radiation treatments.

Radiation Type	Particle Energy (MeV)	Doses (Gy)	Penetration Depth	Irradiation Time (s)
Electron (e^-)	6	$0.5/1.0/5.0 \times 10^4$	all volume	2040-8160
Proton (p^+)	3	$2.5/5.0/10 \times 10^7$	70-90 μm	558-6610

No noticeable changes in the surface roughness of the glasses were observed post-radiation treatment, even at higher doses. Neither expansion nor contraction was detected using a 3D optical profiler. However, the glasses exhibited a darker shade, especially following electron irradiation. Proton irradiation also resulted in a very mild dark coloration, as seen in Figure 19. Figure 19. The most visible square shape, because of a beam mask, is from the phosphate glasses.

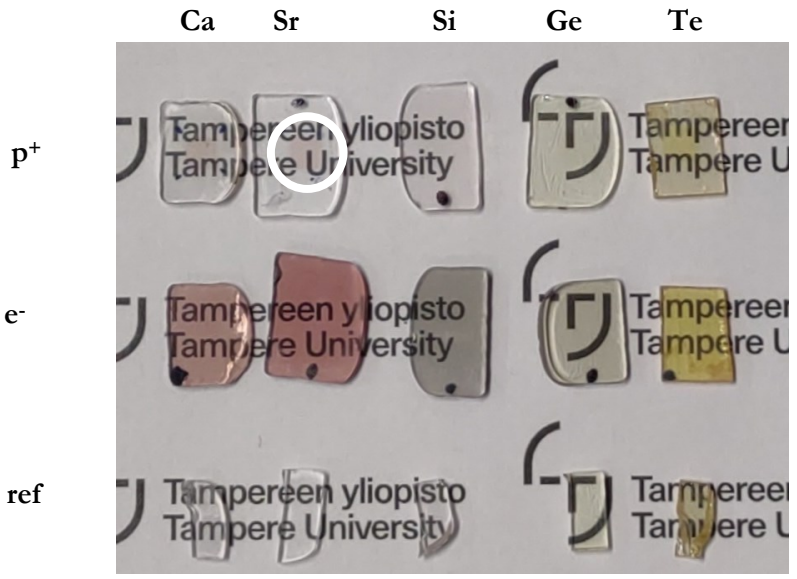

Figure 19. Picture of the investigated glasses prior to (ref) and after irradiation with electrons (e^-) and protons (p^+). Circle shows the proton irradiated area in Sr-phosphate.

The changes in the color of the glasses after irradiation were confirmed from the absorption spectra of the irradiated glasses as seen in Figure 19, new absorption bands appear after the radiation treatment, the intensity of increases as the dosage of electrons and protons rises.

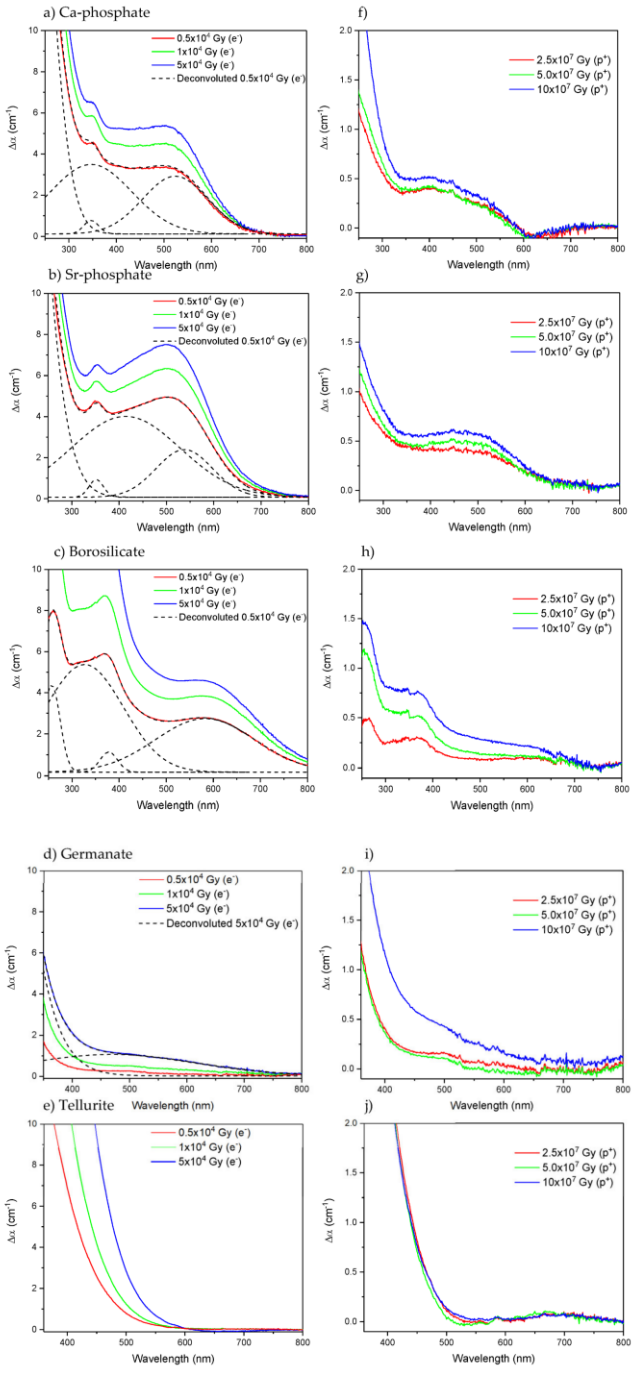

Figure 20. Subtracted absorption spectra prior to and after radiation treatment with electrons (a–e) and proton (f–j) of the Ca-phosphate, Sr-phosphate, borosilicate, germanate, and tellurite, respectively. (a–d) also include one deconvoluted spectrum from the Figure.

These changes in optical properties are likely due to the formation of defects, the nature of which depends on the glass matrix: [**Publication 3**]

Phosphate glasses: phosphorus oxygen hole centers (POHC), as P-related paramagnetic point defects including phosphoryl (PO_3^{2-}), phosphoranyl (PO_4^{4-}), and phosphinyl (PO_2^{2-}) could be contributors to the bands at 210, 240 and 265 nm, respectively. Moreover, the presence of oxygen hole centers (OHC) with an absorption band at 290 nm could also be expected in both Ca and Sr phosphate glasses post-radiation treatment. [64]

Borosilicate glasses: non-bridging oxygen hole centers (NBOHC) and type 2 self-trapped holes (STH2), as well as oxygen-deficient centers (ODC), could be contributors to the bands at 325 and 380 nm. Furthermore, boron-related defects, namely boron bound oxygen hole centers (BOHC), with an expected absorption band around 350–450 nm are expected to form.

Germanate glasses: the shift of the absorption edge towards longer wavelengths is likely due to the formation of germanium-related oxygen vacancy defects and germanium electron centers. A weak absorption band at around 480 nm appeared post-irradiation, possibly linked to the reduction of Ti^{4+} to Ti^{3+} during the radiation process.

Tellurite glasses: the shift of the absorption edge to a longer wavelength might be related to the creation of tellurium-related electron centers and/or hole centers with a strong absorption band at 365 nm.

As seen in Figure 20, a larger number of defects is expected to form in the glasses during the irradiation with electrons as the entire sample volume is irradiated while the protons barely penetrate the glasses. According to Figure 20, the phosphate and borosilicate glasses are expected to be the most sensitive to radiation treatment, probably due to the relative lightness of their atoms whereas the germanate and tellurite glasses appear to be the most resistant as indicated by the small changes in their optical properties after the radiation treatment.

While the radiation treatments had little to no impact on the Yb^{3+} absorption and emission bands of the phosphate and tellurite glasses, the electron radiation treatment slightly influenced the shape of the absorption and emission bands of the borosilicate and germanate glasses as shown below.

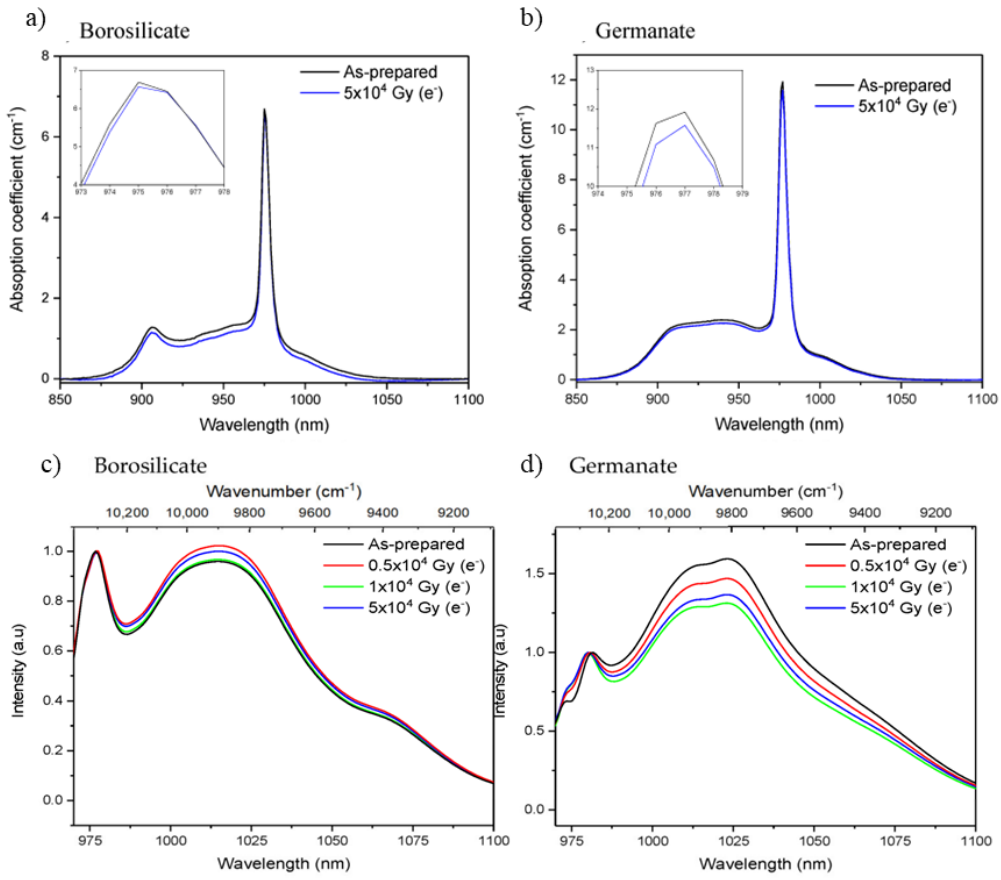

Figure 21. Yb^{3+} absorption band (a-b) and normalized emission band (c-d) for the borosilicate and germanate glasses after electron irradiation showing slight changes.

However, the radiation decreased the Yb^{3+} emission intensity area for all the investigated glasses, except for the tellurite glass. This decrease was more substantial in the borosilicate and germanate glasses. All the changes in the optical and spectroscopic properties of the glasses indicate that the radiation treatment could be affecting the local environment of the Yb^{3+} ions and stabilizing the centers that quench the radiative de-excitation of Yb^{3+} ions.

3.2.3. Recovery of Defects Over Time and After Heat Treatment

Defects formed during radiation treatment are not necessarily permanent and can diminish over time as reported in silicate and phosphate glasses[66], [83]. Here, a

substantial decrease in the absorption coefficient within the 250–500 nm range was observed three months after the irradiation. However, as seen in Figure 22, certain defects remained persistent within the glasses even after this three-month period.

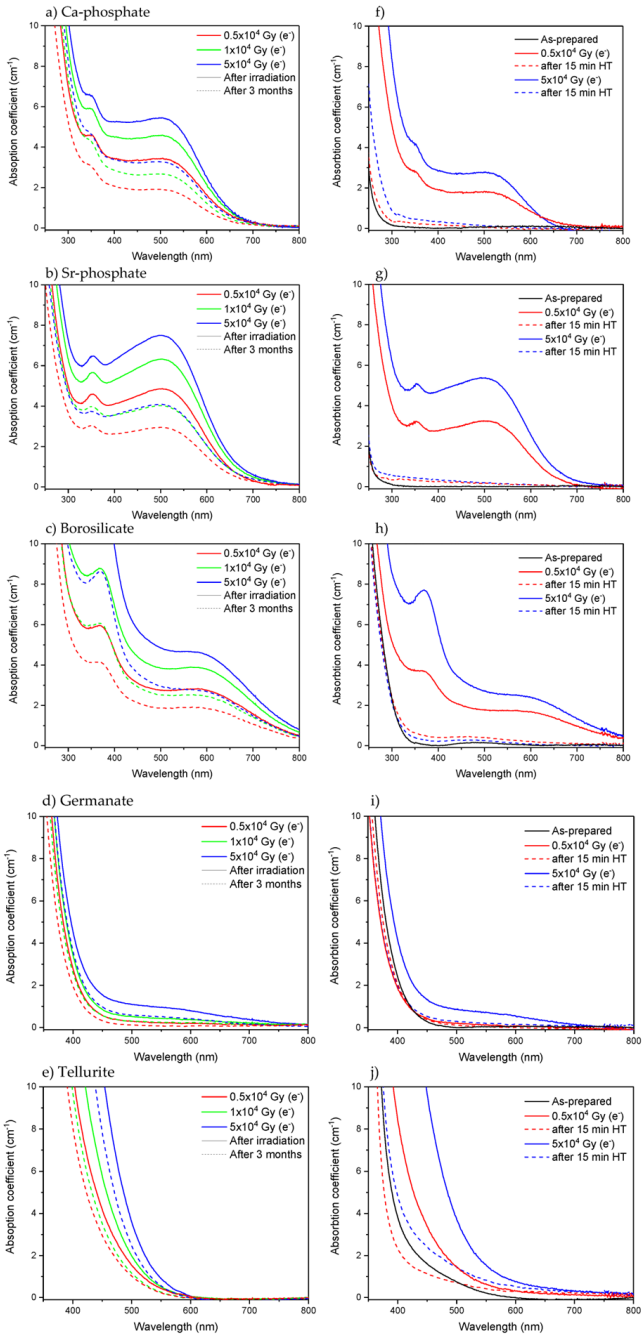

Figure 22. Absorption spectra of Ca-phosphate, Sr-phosphate, borosilicate, germanate, and tellurite glasses measured after irradiation using electrons (solid line), measured 3 months after the irradiation (a–e) and measured after heat treatment (HT) at Tg for 15 min (f–j) (dashed line).

To accelerate the defect recovery process, the irradiated glasses were heat treated at their respective T_g for 15 minutes. This thermal treatment resulted in a drastic reduction of the defects, as evidenced by a >90% decrease in the absorption coefficient within the 250-500 nm range suggesting that the defect formation in the glasses is largely a reversible process. Heat treatment resulted in the Yb^{3+} emission intensity area to increase to the levels observed prior to the irradiation. This restoration of Yb^{3+} emission intensity demonstrates a successful recovery of the optical and spectroscopic properties of the glass after the heat treatment, aligning with previous studies conducted on irradiated phosphate glasses and silica fiber [66], [83].

4.2.3 Conclusions

The effect of radiation treatments on the optical and spectroscopic properties of various Yb^{3+} doped glasses were examined. These findings highlighted the differences in response to radiation among the glasses, with phosphate and borosilicate glasses being the most sensitive, and tellurite glasses showing remarkable resilience. Further investigation into these optical changes could lead to advancements in the design and application of radiation-resistant materials. It was observed that radiation treatments had the potential to significantly alter the absorption properties and create new defect structures, impacting the optical and spectroscopic characteristics of these materials. Notably, the Yb^{3+} emission intensity, a fundamental indicator of the optical performance in lasing, exhibited a decrease in all irradiated glasses except for the tellurite glass. However, these changes were not irreversible. Subsequent examinations following a three-month period after the irradiation revealed a significant spontaneous recovery in the absorption coefficient within the 250–500 nm range, implying a substantial reduction in defect numbers. The potential for defect recovery was further improved using a thermal treatment experiment, demonstrating that most radiation-induced defects can be substantially diminished and the Yb^{3+} emission intensity restored to the level prior to the irradiation. For defect resistant fibers, HMO glasses offer the highest resistance.

4.3 Stability of Yb^{3+} doped glasses in aqueous medium

Although the germanate and tellurite glasses are the most resistant to radiation treatment, these glasses are too difficult to manufacture reliably into novel fibers, not to mention the possible cytotoxicity of the heavy metals. Thus, borosilicate glass was chosen for the development of novel optical fibers. This glass provides good combination of manufacturability and durability. Since the undoped glass has been investigated to have suitable bioactive properties [77], this novel fiber could find uses in biophotonics.

4.3.1 Fiber Manufacturing

The optical fibers were prepared from undoped (clad) and 1.00 mol-% Yb_2O_3 (core) doped borosilicate glass, the composition of which can be found in Table 1. These compositions were selected to fulfill the prerequisite for total internal reflection, which necessitates a higher refractive index for the core glass. These fibers were prepared with different geometries: round and square shapes (Figure 23).

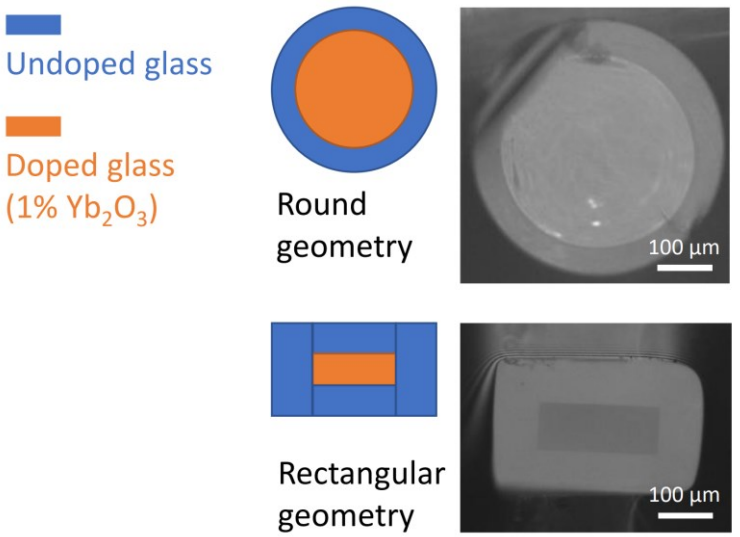

Figure 23. Optical microscope images of the prepared fibers' cross-sections, showcasing the round core-clad and rectangular fibers.

The rectangular and round fibers displayed smooth and defect-free core-cladding interfaces. The general rectangular shape was largely retained during the drawing process, as seen in Figure 23.

Internal characterization of the optical fibers was done through the utilization of X-ray micro computed tomography of the as-drawn fiber, enabling an evaluation of internal homogeneity and geometrical integrity, especially at the core-cladding interfaces. As shown in Figure 24a, the fibers showcased remarkable geometric homogeneity and compositional uniformity, underscoring the success of the novel stack-and-draw method. Interestingly, the tomographic analysis did not detect any significant defects at the core-cladding interface, suggesting that any possible defects were likely to be in the submicron size range, below the detection limit for the tomography. The observed color variation seen in Figure 24a correlates with the X-ray absorption coefficient, reflecting the glass composition. The tomographic analysis on the rectangular fiber bundle revealed the sample's geometric homogeneity and compositional consistency, along with the lack of detectable defects at the core-cladding interface. The diffusion of Yb^{3+} ions from the doped core into the (undoped) cladding was an important aspect in determining the suitability of the stack-and-draw method to prepare core-clad optical fiber for photonics uses. This measurement was achieved by mapping the Yb^{3+} emission using epifluorescent excitation near the core-cladding interface. It is clearly shown that the Yb^{3+} luminescence is confined in the core, with a significant reduction in luminescence over an average thickness of 5 μm at the core-cladding interface. The confinement of Yb^{3+} ions in the core was confirmed using EDS mapping.

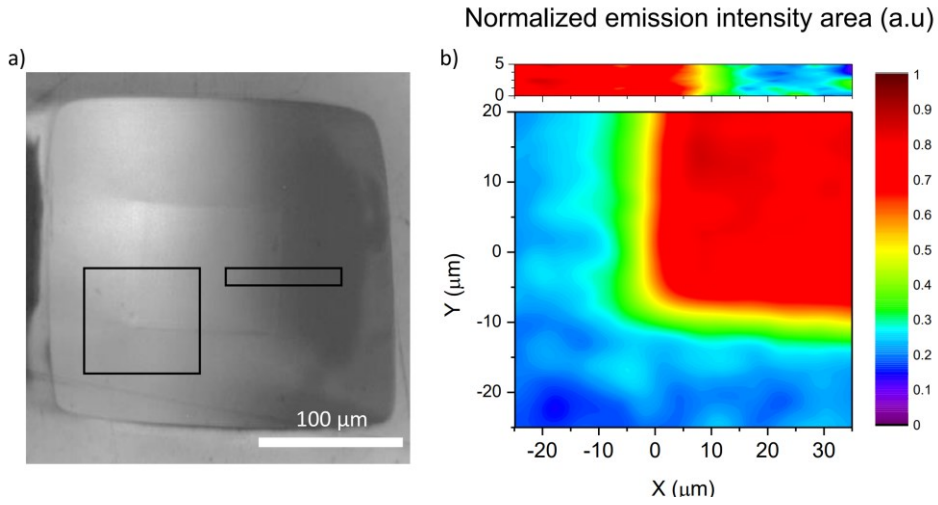

Figure 24. Microscope image of a rectangular fiber (a) and the associated emission mapping (b).

Attenuation measurements, obtained through the cutback method, reveal important characteristics about the transmission properties of the fibers. The measurements demonstrate a minimum loss at wavelengths around 750-800 nm for both fiber types. Beyond this wavelength range, the Yb^{3+} ions present in the core begin to absorb light. At the opposite end of the spectrum, towards the blue region, Rayleigh scattering begins to play a role, further affecting the transmission characteristics. The round fibers have losses of ~8 $dB.m^{-1}$ at 750 nm. While this loss is somewhat high for practical applications, it is expected given the manufacturing process used to prepare the preform. The rectangular fiber, however, shows a significantly higher loss, approximately 30 $dB.m^{-1}$ at 750 nm. One might initially attribute this discrepancy to the difference in core shape, yet comparative studies argue against this, indicating that light leakage does not depend significantly on fiber geometry. Attenuation, in fact, seems to be more closely related to the modes excited or guided within the fiber. This concept is particularly relevant in multimode fibers, where numerous propagation modes coexist within the same fiber, each potentially experiencing different levels of attenuation.

4.3.2 Fiber Stability in Simulated Body Fluid (SBF)

The fiber stability in simulated body fluid (SBF) was investigated over a period of 2 weeks to check if the addition of Yb^{3+} ions in the glass matrix changes the bioresponse of the glass.

As observed for undoped borosilicate glass [77], the pH of the SBF increases overtime due to the leaching of cations into the immersion solution which is a typical occurrence during the dissolution of bioactive glasses within silicate and borosilicate systems. Indeed, using ICP-OES analysis, Si and B were discerned to leach out into the solution, predominantly during the initial 72 hours. However, the ion release rate seemed to slow down after prolonged immersion, indicating the gradual dissolution of the soluble silica and the re-polymerization of the more robust silica network, which then forms an SiO_2-rich gel layer. Boron's behavior in this process was particularly notable. It was primarily released from the glass surface without contributing to the formation of the hydrated layer. This slow-release process was also observed for other elements, such as calcium, which appeared to leach out quickly initially and then stabilize after 72 hours. Conversely, the concentration of

phosphorus in the SBF decreased over time. This simultaneous calcium release and decrease in phosphorus can be associated with the formation of a reactive layer, presumed to be hydroxyapatite, as per the composition of the glass. The behavior of the 1 mol% Yb_2O_3-doped glass mirrors is like the one report for the undoped glass [77] suggesting that the addition of Yb^{3+} ions does not change the precipitation of the hydroxyapatite layer nor the initial dissolution rate of the borosilicate glass.

An experimental setup was designed to track the optical response of a 3-cm-long fiber piece, with 1 cm immersed in SBF over time. This experiment was conducted for fibers of both round core-clad and rectangular core-clad geometries. The transmitted optical powers through the fibers immersed in SBF are depicted in Figure 25.

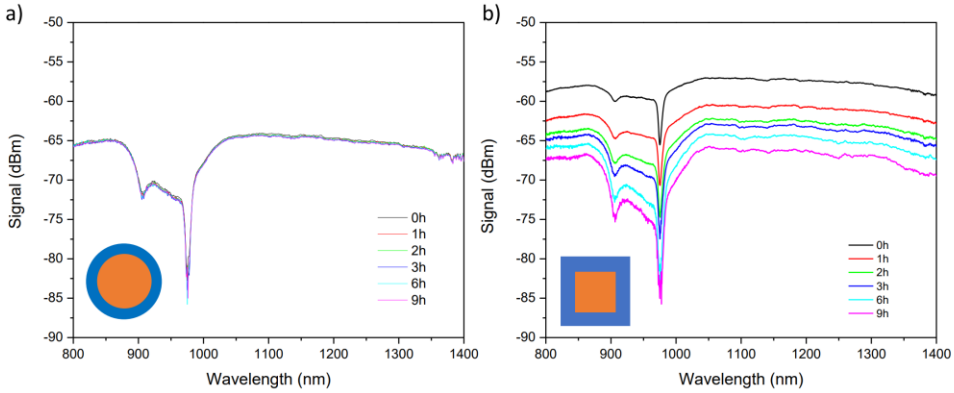

Figure 25. Transmitted optical power through 1-cm piece of fiber in SBF as a function of time for (a) round core-clad and (b) rectangular core-clad geometries.

After a 9-hour immersion period, the rectangular fiber exhibited an increase in losses, while the round fiber transmission remained virtually unchanged. In the round fiber, the light remains confined within the core, and the cladding serves as a buffer layer, effectively preventing interaction between the transmitted light and any surface defects formed. Conversely, the rectangular core-clad fiber appeared to be significantly more susceptible to the aqueous medium, suggesting a less effective protective role of the cladding. SEM images of the round and rectangular core-clad fiber after SBF immersion clearly show that the degradation is vastly different in the two different fiber types, seen in Figure 26.

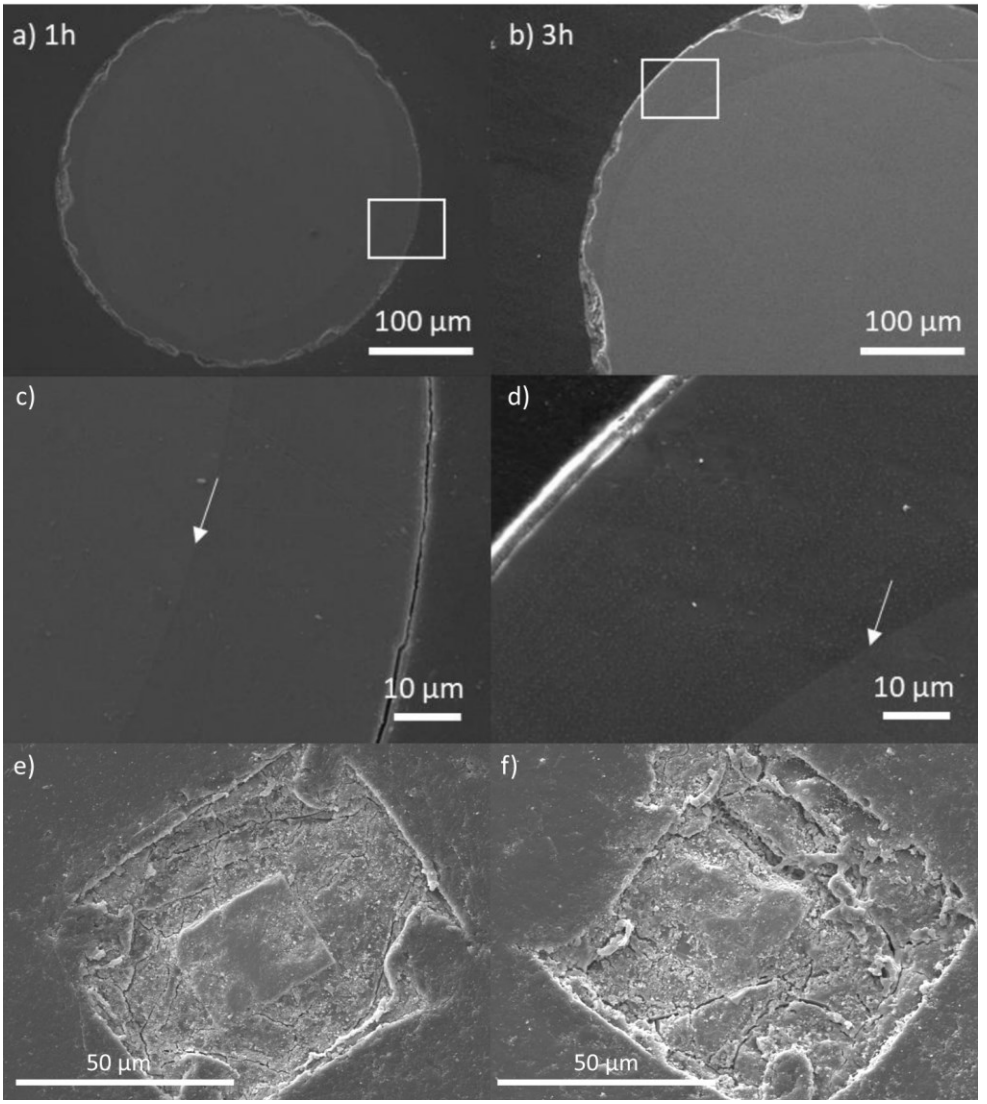

Figure 26. SEM images of the round core-clad fiber after 1h (a), zoomed (c), 3h (b), zoomed (d) and rectangular fiber after 1h (e) and 3h (f).

The phenomenon of stress corrosion cracking (SCC) has been identified as playing a crucial role in the reactivity and overall longevity of glass fibers.[84], [85] The presence of tensile stress within the glass fibers is suspected to lead to an increase in the material's chemical reactivity. Stress distribution within the fibers can be

examined visually, as exemplified in Figure 27: the fringes revealing the stress concentrations within the material. Notably, the external corners of the fibers show pronounced stress concentrations, a crucial observation that has significant implications for the structural integrity and performance of the fibers.

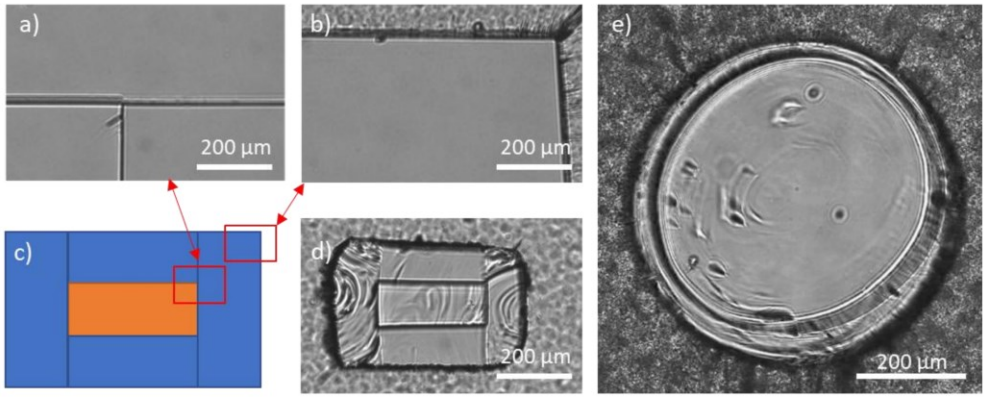

Figure 27. Optical microscope images under polarized light (a) Core-cladding interface and (b) cladding corner of a stacked preform with (c) a schematic diagram showing the locations of both pictures relative to fiber cross-section. (d) Image of the drawn fiber and (e) round fiber. Images taken from samples in epoxy and polished to 400 µm in thickness. Rotating linear polarizers, lighting and focus were adjusted to maximize visibility of the fringes.

Given that tensile stress alters the refractive index of a fiber, this suggests the core of the rectangular fiber to have heterogeneous refractive index. Additionally, this stress distribution is not uniform along the axial direction (z), leading to variable index profiles along the fiber's length. The consequent changes in the index profile could result in intense mode coupling, and the guided energy can subsequently couple to higher order modes, otherwise known as "leaky modes," leading to high losses.

4.3.3 Conclusion

This study aimed to investigate the stability of Yb^{3+} doped glasses in aqueous medium. For this study, round and rectangular bioactive fibers were drawn from both undoped and Yb^{3+} doped borosilicate glasses used as the cladding and core of the fiber, respectively. An exhaustive characterization process determined the fibers' physicochemical, photoluminescence, and dissolution properties. The fibers demonstrated outstanding core-cladding interface quality, with limited diffusion of ytterbium ions from the core to the cladding. This ion confinement, crucial for

photonic applications, was confirmed by emission mapping and SEM imaging. Despite minor diameter ratio variations in round fibers due to the impingement method's imperfections, the fibers remained effective as multimode fibers for research purposes. Here, we demonstrated that the external cross-section profile of the fiber significantly influenced their biodegradation behavior, underlining the impact of fiber design on the resultant material's functionality. Rectangular fibers exhibited high losses (approximately 30 dB/m at 800 nm) and accelerated degradation compared to circular ones due to residual tensile stresses induced during fiber drawing. A stress concentration analysis revealed tensile stress presence at rectangular external corners of the fibers, affecting their chemical reactivity and structural integrity. These results suggest the importance of fiber geometry in the degradation behavior of fiber, necessitating careful design and fabrication for application-specific biodegradation optimization. Additional study involving core geometry, specific numerical aperture, diameter, and accounting for mode coupling could be the focus of future comprehensive research.

5 CONCLUSIONS

This thesis provides a comprehensive investigation into modifying the properties of Yb^{3+}-doped glasses through compositional variations and post-processing treatments such as thermal and radiation treatments as well of immersion in aqueous medium. New Yb^{3+}-doped oxyfluorophosphate glasses and glass-ceramics were developed and characterized to gain fundamental insights on glass crystallization in the sodium oxyfluorophosphate system. The research also provided information of defect resistance of different glass types upon radiation treatment and led to development of novel bioactive fibers, the emission of which could be used to track the dissolution of the fiber in the aqueous medium.

With this research, the following questions were answered:

> *How does the addition of fluorine affect Yb^{3+} -doped phosphate glass crystallization? What effects do controlled heat treatments have on crystallization and emission spectra of the Yb^{3+} -doped oxyfluorophosphate glasses? How does the incorporation of Al_2O_3, ZnO and/or TiO_2 in this glass network influence the glass network connectivity and the resistance of the glass to water absorption? How would it change its nucleation and growth mechanism? Can water resistance be optimized without compromising other attributes?*

Precise control over glass composition enables tailoring important material characteristics. Transparent glass-ceramics with increased Yb^{3+}-emission bandwidth were obtained by heat treating phosphate glasses in the $NaPO_3$-Na_2O system with different fluoride concentrations. The effects of fluoride content and heat treatments on crystallization and emission spectra were systematically examined. This revealed how controlled nucleation and crystal growth could be achieved to engineer optical properties for lasers and amplifiers (**Publication 1**). However, the resultant glasses suffered from hygroscopicity, limiting applications. Incorporating minor additions of aluminum oxide, titanium oxide, and zinc oxide was shown to successfully enhance water resistance without hindering other attributes like crystallization behavior and emission characteristics. This work established that network connectivity could be strengthened through appropriate oxide additions to improve stability while maintaining spectroscopic performance (**Publication 2**).

> *How do different glass families (silicates, phosphates, borate, tellurite, etc.) compare in their susceptibility to radiation-induced formation of color centers and microstructural*

changes? Can glass compositions be identified so that the glass exhibit tailored (high/low) radiation tolerances? How do post-processing techniques like thermal treatment influence defect recovery?

Different glass families, including phosphate, borosilicate, germanate, and tellurite compositions, were subjected to radiation treatments. Their defects formation susceptibility and recovery responses were evaluated and compared. Phosphate and borosilicate glasses exhibited the highest initial radiation sensitivity but also demonstrated self-recovery of defects upon heat treatment. In contrast, tellurite glasses exhibited the lowest defect formation, highlighting opportunities for radiation tolerant optical materials (**Publication 3**).

How does glass geometry and fabrication conditions impact degradation kinetics of ytterbium-doped borosilicate fibers in aqueous medium? Can the Yb^{3+} spectroscopic properties be used to track the degradation of the fiber in aqueous medium?

The stability of Yb^{3+}-doped borosilicate glass fibers fabricated in round and rectangular geometries was evaluated in aqueous solution. By monitoring Yb^{3+}-emission over time, the impact of fiber geometry on degradation kinetics was elucidated. This work emphasized that fiber design is crucial for controlling resorption behavior tailored to specific biomedical therapy applications (**Publication 4**).

From the obtained results, new and intriguing future opportunities for continued research emerge:

- Transparent Yb^{3+}-doped glass-ceramics with increased emission bandwidth were obtained. Additional work could explore upscaling glass-ceramic production and perform characterization relevant to actual laser/amplifier device engineering. Incorporating network-forming oxides successfully enhanced glass stability but also influenced crystallization. A deeper examination of these structure-property tradeoffs could provide design guidelines for optimizing both attributes simultaneously.
- Resistance of different glass types against radiation induced defects was studied. Further research could focus on adjusting defect resistance with other alkali/alkali-earth modifiers, such as potassium or barium. Additionally, the exact mechanism of the observed Yb^{3+} emission reduction in germanate glasses could be of interest as it proved to be highly resistant to light absorbing defects.
- Fiber geometry significantly impacted the biodegradation behavior of Yb^{3+}-doped borosilicate glass fibers. More research is warranted to improve the stack and drawn technique to reduce stress concentration at rectangular external

corners of the fibers for the development of fiber with unique designs tailored for specific resorption timescales in biomedical therapies.

Altogether, this in-depth study has significantly advanced fundamental comprehension on how compositional modifications and thermal/radiation processes can modulate performance attributes of Yb^{3+} doped glass-based material. These findings offer new strategies and design principles for optimizing desirable traits such as emission bandwidth, chemical and thermal stability, radiation tolerance, and dissolution profiles. This improved understanding supports the continued advancement and broader utilization of versatile glass-based technologies. The methods and insights developed in this work lay the groundwork for additional optimization and exploration of glass systems. It provides a foundation to inspire new investigations aiming to push the boundaries of glass-based materials for applications in photonics, healthcare, radiation detection, and beyond.

6 REFERENCES

[1] J. E. Shelby, "Introduction to Glass Science and Technology," *Introduction to Glass Science and Technology*, Jan. 2005, doi: 10.1039/9781847551160.

[2] W. H. Zachariasen, "The atomic arrangement in glass," *J Am Chem Soc*, vol. 54, no. 10, pp. 3841–3851, Oct. 1932, doi: 10.1021/JA01349A006/ASSET/JA01349A006.FP.PNG_V03.

[3] M. Ojansivu *et al.*, "The effect of S53P4-based borosilicate glasses and glass dissolution products on the osteogenic commitment of human adipose stem cells," *PLoS One*, vol. 13, no. 8, p. e0202740, Aug. 2018, doi: 10.1371/JOURNAL.PONE.0202740.

[4] L. L. Hench, "The story of Bioglass®," *J Mater Sci Mater Med*, vol. 17, no. 11, pp. 967–978, Nov. 2006, doi: 10.1007/S10856-006-0432-Z/METRICS.

[5] A. Hoppe, N. S. Güldal, and A. R. Boccaccini, "A review of the biological response to ionic dissolution products from bioactive glasses and glass-ceramics," *Biomaterials*, vol. 32, no. 11, pp. 2757–2774, Apr. 2011, doi: 10.1016/J.BIOMATERIALS.2011.01.004.

[6] A. Lemiere, B. Bondzior, B. Bondzior, L. Kuusela, A. Veber, and L. Petit, "Spectroscopic properties of $Er^{3+;}$ doped germanate glasses before and after a heat treatment process," *Optical Materials Express, Vol. 13, Issue 1, pp. 218-228*, vol. 13, no. 1, pp. 218–228, Jan. 2023, doi: 10.1364/OME.476131.

[7] J. de Clermont-Gallerande, S. Saito, M. Colas, P. Thomas, and T. Hayakawa, "New understanding of TeO_2–ZnO–Na_2O ternary glass system," *J Alloys*

Compd, vol. 854, p. 157072, Feb. 2021, doi: 10.1016/J.JALLCOM.2020.157072.

[8] M. Yamane and Y. Asahara, "Glasses for Photonics," *Glasses for Photonics*, May 2000, doi: 10.1017/CBO9780511541308.

[9] S. Świontek, M. Środa, and W. Gieszczyk, "Ceramics, Glass and Glass-Ceramics for Personal Radiation Detectors," *Materials 2021, Vol. 14, Page 5987*, vol. 14, no. 20, p. 5987, Oct. 2021, doi: 10.3390/MA14205987.

[10] N. Ojha, A. Szczodra, N. G. Boetti, J. Massera, and L. Petit, "Nucleation and growth behavior of Er^{3+} doped oxyfluorophosphate glasses," *RSC Adv*, vol. 10, no. 43, pp. 25703–25716, Jul. 2020, doi: 10.1039/D0RA04681G.

[11] A. Moguš-Milanković, A. Gajović, A. Šantić, and D. E. Day, "Structure of sodium phosphate glasses containing Al_2O_3 and/or Fe_2O_3. Part I," *J Non Cryst Solids*, vol. 289, no. 1–3, pp. 204–213, Aug. 2001, doi: 10.1016/S0022-3093(01)00701-3.

[12] H. Liu, R. Yang, Y. Wang, and S. Liu, "Influence of Alumina Additions on the Physical and Chemical Properties of Lithium-iron-phosphate Glasses," *Phys Procedia*, vol. 48, pp. 17–22, Jan. 2013, doi: 10.1016/J.PHPRO.2013.07.004.

[13] R. K. Brow, "Nature of Alumina in Phosphate Glass: I, Properties of Sodium Aluminophosphate Glass," *Journal of the American Ceramic Society*, vol. 76, no. 4, pp. 913–918, Apr. 1993, doi: 10.1111/j.1151-2916.1993.tb05315.x.

[14] O. Kalwasińska *et al.*, "The effect of titanium dioxide addition on physical and biological properties of Na_2O-B_2O_3-P_2O_5 and CaO-Na_2O-P_2O_5 glasses," *Engineering of Biomaterials*, no. Vol. 19, 134, pp. 2--7, 2016

[15] E. A. Abou Neel, W. Chrzanowski, and J. C. Knowles, "Effect of increasing titanium dioxide content on bulk and surface properties of phosphate-based glasses," *Acta Biomater*, vol. 4, no. 3, pp. 523–534, 2008, doi: 10.1016/J.ACTBIO.2007.11.007.

[16] L. E. Bausá, J. García Solé, A. Durán, and J. M. Fernández Navarro, "Characterization of titanium induced optical absorption bands in phosphate glasses," *J Non Cryst Solids*, vol. 127, no. 3, pp. 267–272, Feb. 1991, doi: 10.1016/0022-3093(91)90479-P.

[17] E. A. Abou Neel *et al.*, "Doping of a high calcium oxide metaphosphate glass with titanium dioxide," *J Non Cryst Solids*, vol. 355, no. 16–17, pp. 991–1000, Jun. 2009, doi: 10.1016/j.jnoncrysol.2009.04.016.

[18] M. M. Babu *et al.*, "Titanium incorporated Zinc-Phosphate bioactive glasses for bone tissue repair and regeneration: Impact of Ti^{4+}on physico-mechanical and in vitro bioactivity," *Ceram Int*, vol. 45, no. 17, pp. 23715–23727, Dec. 2019, doi: 10.1016/j.ceramint.2019.08.087.

[19] A. V. DeCeanne, L. R. Rodrigues, C. J. Wilkinson, J. C. Mauro, and E. D. Zanotto, "Examining the role of nucleating agents within glass-ceramic systems," *J Non Cryst Solids*, vol. 591, p. 121714, Sep. 2022, doi: 10.1016/J.JNONCRYSOL.2022.121714.

[20] R. Oueslati-Omrani and A. H. Hamzaoui, "Effect of ZnO incorporation on the structural, thermal and optical properties of phosphate based silicate glasses," *Mater Chem Phys*, vol. 242, p. 122461, Feb. 2020, doi: 10.1016/J.MATCHEMPHYS.2019.122461.

[21] B. P. Choudhary, S. Rai, and N. B. Singh, "Properties of silver phosphate glass doped with nanosize zinc oxide," *Ceram Int*, vol. 42, no. 9, pp. 10813–10825, Jul. 2016, doi: 10.1016/J.CERAMINT.2016.03.210.

[22] R. K. Brow, D. R. Tallant, S. T. Myers, and C. C. Phifer, "The short-range structure of zinc polyphosphate glass," *J Non Cryst Solids*, vol. 191, no. 1–2, pp. 45–55, 1995, doi: 10.1016/0022-3093(95)00289-8.

[23] T. R. Stechert, M. J. D. Rushton, and R. W. Grimes, "Predicted Mechanism for Enhanced Durability of Zinc Containing Silicate Glasses," *Journal of the American Ceramic Society*, vol. 96, no. 5, pp. 1450–1455, May 2013, doi: 10.1111/jace.12308.

[24] N. Kanwal *et al.*, "Structure and solubility behaviour of zinc containing phosphate glasses," *J Mater Chem B*, vol. 3, no. 45, pp. 8842–8855, Nov. 2015, doi: 10.1039/C4TB01504E.

[25] "File:Simple Periodic Table Chart-blocks.svg - Wikimedia Commons." Accessed: Sep. 03, 2023. [Online]. Available: https://commons.wikimedia.org/wiki/File:Simple_Periodic_Table_Chart-blocks.svg

[26] K. Soga, "Glass and biophotonics," *Journal of the Ceramic Society of Japan*, vol. 130, no. 8, pp. 590–594, Aug. 2022, doi: 10.2109/JCERSJ2.22036.

[27] L. Marcu, S. A. Boppart, M. R. Hutchinson, J. Popp, and B. C. Wilson, "Biophotonics: the big picture," *https://doi-org.libproxy.tuni.fi/10.1117/1.JBO.23.2.021103*, vol. 23, no. 2, p. 021103, Dec. 2017, doi: 10.1117/1.JBO.23.2.021103.

[28] W. Höland and G. H. Beall, "Glass-ceramic technology," *Glass-Ceramic Technology*, pp. 1–422, Jan. 2019, doi: 10.1002/9781119423737.

[29] L. Fu, H. Engqvist, and W. Xia, "Glass–Ceramics in Dentistry: A Review," *Materials 2020, Vol. 13, Page 1049*, vol. 13, no. 5, p. 1049, Feb. 2020, doi: 10.3390/MA13051049.

[30] A. S. Myerson, D. Erdemir, and A. Y. Lee, "Crystal Nucleation," *Handbook of Industrial Crystallization*, pp. 76–114, Jan. 2019, doi: 10.1017/9781139026949.003.

[31] J. W. P. Schmelzer, A. S. Abyzov, V. M. Fokin, C. Schick, and E. D. Zanotto, "Crystallization of glass-forming liquids: Maxima of nucleation, growth, and overall crystallization rates," *J Non Cryst Solids*, vol. 429, pp. 24–32, Dec. 2015, doi: 10.1016/J.JNONCRYSOL.2015.08.023.

[32] D. Gebauer, M. Kellermeier, J. D. Gale, L. Bergström, and H. Cölfen, "Pre-nucleation clusters as solute precursors in crystallisation," *Chem Soc Rev*, vol. 43, no. 7, pp. 2348–2371, Mar. 2014, doi: 10.1039/C3CS60451A.

[33] Q. Pan *et al.*, "Engineering Tunable Broadband Near-Infrared Emission in Transparent Rare-Earth Doped Nanocrystals-in-Glass Composites via a Bottom-Up Strategy," *Adv Opt Mater*, vol. 7, no. 6, p. 1801482, Mar. 2019, doi: 10.1002/ADOM.201801482.

[34] Q. Pan *et al.*, "Engineering Tunable Broadband Near-Infrared Emission in Transparent Rare-Earth Doped Nanocrystals-in-Glass Composites via a Bottom-Up Strategy," *Adv Opt Mater*, vol. 7, no. 6, p. 1801482, Mar. 2019, doi: 10.1002/ADOM.201801482.

[35] M. Simoncelli, N. Marzari, and F. Mauri, "Unified theory of thermal transport in crystals and glasses," *Nature Physics 2019 15:8*, vol. 15, no. 8, pp. 809–813, May 2019, doi: 10.1038/s41567-019-0520-x.

[36] N. Terakado, T. Yoshimine, R. Kozawa, Y. Takahashi, and T. Fujiwara, "Transparent glass-ceramics for thermal management application: achievement of optical transparency and high thermal conductivity," *RSC Adv*, vol. 10, no. 38, pp. 22352–22360, Jun. 2020, doi: 10.1039/D0RA03026K.

[37] P. D. Dragic, M. Cavillon, and J. Ballato, "Materials for optical fiber lasers: A review," *Appl Phys Rev*, vol. 5, no. 4, p. 041301, Oct. 2018, doi: 10.1063/1.5048410.

[38] W. F. Krupke, "Ytterbium solid-state lasers - the first decade," *IEEE Journal on Selected Topics in Quantum Electronics*, vol. 6, no. 6, pp. 1287–1296, Nov. 2000, doi: 10.1109/2944.902180.

[39] V. Venkatramu *et al.*, "Optical properties of Yb^{3+}-doped phosphate laser glasses," *J Alloys Compd*, vol. 509, no. 16, pp. 5084–5089, Apr. 2011, doi: 10.1016/j.jallcom.2011.01.148.

[40] Y. Mao, P. Deng, F. Gan, H. Yang, and W. Shen, "Spectroscopic properties of ytterbium in phosphate glass," *Mater Lett*, vol. 57, no. 2, pp. 439–443, Dec. 2002, doi: 10.1016/S0167-577X(02)00807-8.

[41] J. Limpert *et al.*, "High-power femtosecond Yb-doped fiber amplifier," *Opt Express*, vol. 10, no. 14, p. 628, Jul. 2002, doi: 10.1364/oe.10.000628.

[42] M. E. Likhachev *et al.*, "Large-mode-area highly Yb-doped photodarkening-free Al_2O_3-P_2O_5-SiO_2-Based fiber," in *2011 Conference on Lasers and Electro-Optics Europe and 12th European Quantum Electronics Conference, CLEO EUROPE/EQEC 2011*, 2011. doi: 10.1109/CLEOE.2011.5943202.

[43] S. Q. Xu *et al.*, "Thermal stability and spectroscopic properties of Yb3+-doped new gallium-lead-germanate glass," *Chinese Physics Letters*, vol. 23, no. 11, p. 3069, Nov. 2006, doi: 10.1088/0256-307X/23/11/051.

[44] C. Jiang, P. Deng, J. Zhang, G. Huang, and F. Gan, "Yb : Tellurogermanate laser glass with high emission cross section," *J Lumin*, vol. 82, no. 4, pp. 321–326, 1999, doi: 10.1016/S0022-2313(99)00049-6.

[45] J. Thomas *et al.*, "Optical properties of ytterbium doped oxyfluoride glass-ceramics - Concentration and temperature dependence studies for optical refrigeration applications," *J Lumin*, vol. 238, p. 118278, Oct. 2021, doi: 10.1016/J.JLUMIN.2021.118278.

[46] D. Chen *et al.*, "Dual-Phase Glass Ceramic: Structure, Dual-Modal Luminescence, and Temperature Sensing Behaviors," *ACS Appl Mater Interfaces*, vol. 7, no. 34, pp. 19484–19493, Aug. 2015, doi: 10.1021/ACSAMI.5B06036/ASSET/IMAGES/MEDIUM/AM-2015-06036Q_0006.GIF.

[47] S. Ye *et al.*, "Enhanced cooperative quantum cutting in Tm^{3+}-Yb^{3+} codoped glass ceramics containing LaF_3 nanocrystals," *Optics Express, Vol. 16, Issue 12, pp. 8989-8994*, vol. 16, no. 12, pp. 8989–8994, Jun. 2008, doi: 10.1364/OE.16.008989.

[48] G. Dantelle, M. Mortier, D. Vivien, and G. Patriarche, "Nucleation efficiency of erbium and ytterbium fluorides in transparent oxyfluoride glass-ceramics," *J Mater Res*, vol. 20, no. 2, pp. 472–481, Feb. 2005, doi: 10.1557/JMR.2005.0051/METRICS.

[49] G. Dantelle, M. Mortier, P. Goldner, and D. Vivien, "EPR and optical study of Yb^{3+}-doped β-PbF_2 single crystals and nanocrystals of glass-ceramics," *Journal of Physics: Condensed Matter*, vol. 18, no. 34, p. 7905, Aug. 2006, doi: 10.1088/0953-8984/18/34/005.

[50] "File:Optical-fibre.png - Wikimedia Commons." Accessed: Sep. 03, 2023. [Online]. Available: https://commons.wikimedia.org/wiki/File:Optical-fibre.png

[51] T. K. Gangopadhyay, P. Kumbhakar, and M. K. Mandal, *Photonics and fiber optics : foundations and applications*.

[52] T. Sagawa, R. Kobayashi, A. Utsumi, T. Sugawa, and T. Shintani, "Modified rod-in-tube method for low- loss step-index optical fiber," *Optical Fiber Communication (1979), paper WF1*, p. WF1, Mar. 1979, doi: 10.1364/OFC.1979.WF1.

[53] L. Kociszewski, J. Buzniak, R. Stepien, and R. S. Romaniuk, "Optical Devices And Sensors Made Of Special-Purpose Fibers," vol. 0867, pp. 122–129, Jun. 1988, doi: 10.1117/12.965071.

[54] C. Strutynski *et al.*, "Stack-and-Draw Applied to the Engineering of Multi-Material Fibers with Non-Cylindrical Profiles," *Adv Funct Mater*, vol. 31, no. 22, p. 2011063, May 2021, doi: 10.1002/ADFM.202011063.

[55] S. Heyvaert, H. Ottevaere, I. Kujawa, R. Buczynski, and H. Thienpont, "Stack-and-draw technique creates ultrasmall-diameter endoscopes," *Laser Focus World*, vol. 49, no. 12, Endeavor Business Media, Tulsa, pp. 29–30, 32, 34–35

[56] L. Kociszewski, J. Buzniak, R. Stepien, and R. S. Romaniuk, "Optical Devices And Sensors Made Of Special-Purpose Fibers", vol. 0867, pp. 122–129, Jun. 1988, doi: 10.1117/12.965071.

[57] C. D. Hussey, "Glass: Optical Fibers – Manufacture and Properties," *Encyclopedia of Materials: Technical Ceramics and Glasses*, vol. 2–3, pp. 681–688, Jan. 2021, doi: 10.1016/B978-0-12-818542-1.00019-9.

[58] S. Abrate, R. Gaudino, G. Perrone, S. Abrate, R. Gaudino, and G. Perrone, "Step-Index PMMA Fibers and Their Applications," *Current Developments in Optical Fiber Technology*, Jun. 2013, doi: 10.5772/52746.

[59] R. Tao, X. Wang, and P. Zhou, "Comprehensive Theoretical Study of Mode Instability in High-Power Fiber Lasers by Employing a Universal Model and Its Implications," *IEEE Journal of Selected Topics in Quantum Electronics*, vol. 24, no. 3, May 2018, doi: 10.1109/JSTQE.2018.2811909.

[60] Z. M. Ziegler, L. G. Wright, F. W. Wise, and Z. Liu, "Megawatt peak power from a Mamyshev oscillator," *Optica, Vol. 4, Issue 6, pp. 649-654*, vol. 4, no. 6, pp. 649–654, Jun. 2017, doi: 10.1364/OPTICA.4.000649.

[61] W. Peng, Z. Fang, Z. Ma, and J. Qiu, "Enhanced upconversion emission in crystallization-controllable glass-ceramic fiber containing Yb^{3+}-Er^{3+} codoped CaF_2 nanocrystals," *Nanotechnology*, vol. 27, no. 40, p. 405203, Aug. 2016, doi: 10.1088/0957-4484/27/40/405203.

[62] J. Ballato *et al.*, "Laser cooling in a silica optical fiber at atmospheric pressure," *Optics Letters, Vol. 45, Issue 5, pp. 1092-1095*, vol. 45, no. 5, pp. 1092–1095, Mar. 2020, doi: 10.1364/OL.384658.

[63] L. Skuja, M. Hirano, H. Hosono, and K. Kajihara, "Defects in oxide glasses," *physica status solidi (c)*, vol. 2, no. 1, pp. 15–24, 2005, doi: 10.1002/pssc.200460102.

[64] D. Möncke and D. Ehrt, "Irradiation induced defects in glasses resulting in the photoionization of polyvalent dopants," *Opt Mater (Amst)*, vol. 25, no. 4, pp. 425–437, May 2004, doi: 10.1016/J.OPTMAT.2003.11.001.

[65] S. Girard *et al.*, "Overview of radiation induced point defects in silica-based optical fibers," *Reviews in Physics*, vol. 4. Elsevier B.V., p. 100032, Nov. 01, 2019. doi: 10.1016/j.revip.2019.100032.

[66] D. Möncke, J. Jiusti, L. D. Silva, and A. C. M. Rodrigues, "Long-term stability of laser-induced defects in (fluoride-)phosphate glasses doped with W, Mo, Ta, Nb and Zr ions," *J Non Cryst Solids*, vol. 498, pp. 401–414, Oct. 2018, doi: 10.1016/J.JNONCRYSOL.2018.03.004.

[67] C. Shao *et al.*, "193 nm excimer laser-induced color centers in $Yb^{3+}/Al^{3+}/P^{5+}$-doped silica glasses," *J Non Cryst Solids*, vol. 544, p. 120198, Sep. 2020, doi: 10.1016/J.JNONCRYSOL.2020.120198.

[68] A. A. Rybaltovsky *et al.*, "Role of oxygen hole centres in the photodarkening of ytterbium-doped phosphosilicate fibre," *Quantum Elec (Woodbury)*, vol. 43, no. 11, pp. 1037–1042, Nov. 2013, doi: 10.1070/QE2013V043N11ABEH015216/XML.

[69] M. Leich, J. Kirchhof, S. Jetschke, and S. Unger, "Photodarkening kinetics as a function of Yb concentration and the role of Al codoping," *Applied Optics, Vol. 51, Issue 32, pp. 7758-7764*, vol. 51, no. 32, pp. 7758–7764, Nov. 2012, doi: 10.1364/AO.51.007758.

[70] D. Möncke and D. Ehrt, "Photoionization of Polyvalent Ions," in *Photoionization of Polyvalent Ions*, Nova Science Publishers, Inc., 2009, pp. 1–82.

[71] P. Jelger, F. Laurell, M. Engholm, and L. Norin, "Improved photodarkening resistivity in ytterbium-doped fiber lasers by cerium codoping," *Optics Letters, Vol. 34, Issue 8, pp. 1285-1287*, vol. 34, no. 8, pp. 1285–1287, Apr. 2009, doi: 10.1364/OL.34.001285.

[72] L. Petit, "Radiation effects on phosphate glasses: Review," *Int J Appl Glass Sci*, vol. 11, no. 3, pp. 511–521, Jul. 2020, doi: 10.1111/IJAG.14075.

[73] Jantzen, C. M. Historical development of glass and ceramic waste forms for high level radioactive wastes. In *Handbook of Advanced Radioactive Waste Conditioning Technologies*. (ed Ojovan, M. I.) Ch. 6, 159–172 (Woodhead, 2011).

[74] M. Hongisto *et al.*, "Radiation-Induced Defects and Effects in Germanate and Tellurite Glasses," *Materials 2020, Vol. 13, Page 3846*, vol. 13, no. 17, p. 3846, Aug. 2020, doi: 10.3390/MA13173846.

[75] J. P. Celli *et al.*, "Imaging and photodynamic therapy: Mechanisms, monitoring, and optimization," *Chem Rev*, vol. 110, no. 5, pp. 2795–2838, May 2010, doi: 10.1021/CR900300P/ASSET/IMAGES/MEDIUM/CR-2009-00300P_0043.GIF.

[76] S. H. Mussavi Rizi, N. G. Boetti, D. Pugliese, and D. Janner, "Phosphate glass-based microstructured optical fibers with hole and core for biomedical applications," *Opt Mater (Amst)*, vol. 131, p. 112644, Sep. 2022, doi: 10.1016/J.OPTMAT.2022.112644.

[77] M. Ojansivu *et al.*, "The effect of S53P4-based borosilicate glasses and glass dissolution products on the osteogenic commitment of human adipose stem cells," *PLoS One*, vol. 13, no. 8, p. e0202740, Aug. 2018, doi: 10.1371/JOURNAL.PONE.0202740.

[78] J. Massera *et al.*, "Effect of the glass melting condition on the processing of phosphate-based glass–ceramics with persistent luminescence properties," *Opt Mater (Amst)*, vol. 52, pp. 56–61, Feb. 2016, doi: 10.1016/J.OPTMAT.2015.12.006.

[79] M. Hongisto, "Advanced particle containing glasses for photonics," Aug. 2019, Accessed: Oct. 12, 2023. [Online]. Available: https://trepo.tuni.fi/handle/10024/116784

[80] R. Hui and M. O'Sullivan, "Fiber Optic Measurement Techniques," *Fiber Optic Measurement Techniques*, pp. 1–652, Jan. 2008, doi: 10.1016/B978-0-12-373865-3.X0001-8.

[81] R. Ternane, M. Ferid, Y. Guyot, M. Trabelsi-Ayadi, and G. Boulon, "Spectroscopic properties of Yb^{3+} in $NaYbP_2O_7$ diphosphate single crystals," *J Alloys Compd*, vol. 464, no. 1–2, pp. 327–331, Sep. 2008, doi: 10.1016/J.JALLCOM.2007.09.104.

[82] H. Ohkawa, H. Hayashi, and Y. Kondo, "Influence of water on non-radiative decay of Yb^{3+}–$^2F_{5/2}$ level in phosphate glass," *Opt Mater (Amst)*, vol. 33, no. 2, pp. 128–130, Dec. 2010, doi: 10.1016/J.OPTMAT.2010.10.027.

[83] D. Möncke and D. Ehrt, "Irradiation induced defects in glasses resulting in the photoionization of polyvalent dopants," *Opt Mater (Amst)*, vol. 25, no. 4, pp. 425–437, May 2004, doi: 10.1016/j.optmat.2003.11.001.

[84] D. Li, F. Yang, and J. Nychka, "Indentation-induced residual stresses in 45S5 bioglass and the stress effect on the material dissolution," *Eng Fract Mech*, vol. 75, no. 17, pp. 4898–4908, Nov. 2008, doi: 10.1016/J.ENGFRACMECH.2008.06.024.

[85] J. Yu, Q. Jian, W. Yuan, B. Gu, F. Ji, and W. Huang, "Further damage induced by water in micro-indentations in phosphate laser glass," *Appl Surf Sci*, vol. 292, pp. 267–277, Feb. 2014, doi: 10.1016/J.APSUSC.2013.11.129.

Développement de verres et vitrocéramiques dopés ytterbium pour l'optique et réponses sous différents types de traitements

Résumé

Ce travail de thèse propose une étude sur la modification des propriétés des composés vitreux dopés par des ions $Yb^{3+,}$ à travers des variations de composition, de traitements thermiques ou par rayonnement ainsi que par immersion en milieu aqueux. De nouveaux verres/vitrocéramique type oxyfluorophosphate dopés Yb^{3+} ont été développés et caractérisés pour obtenir des informations fondamentales sur la cristallisation. L'étude propose également le développement de fibres bioactives cylindriques et rectangulaires à base de verre borosilicate dopées et non dopées constituant respectivement le cœur et la gaine de la fibre. La stabilité de ces fibres en milieu aqueux est suivie en fonction de la géométrie. Cette étude fournit également des informations sur la résistance aux défauts en fonction de la nature du réseau et sur le développement de nouvelles fibres bioactives, dont l'émission pourrait être utilisée pour suivre la dissolution de la fibre dans le milieu aqueux. Cette étude contribue à une meilleure compréhension fondamentale sur la façon dont les modifications de composition et les processus thermiques / de rayonnement peuvent moduler les paramètres de performance des matériaux vitreux dopés par des ions $Yb^{3+.}$

Mots clés: Vitrocéramiques, ytterbium, matériaux bioactifs

Development of ytterbium-doped optical glasses and glassceramics and their response to various treatments

Abstract

This thesis studies the modification of the properties of glass compounds doped with Yb^{3+} ions, through variations in composition, thermal or radiation treatments as well as by immersion in aqueous medium. New Yb^{3+} doped oxyfluorophosphate glass/glass-ceramics have been developed and characterized to obtain fundamental information on crystallization. The study also proposes the development of cylindrical and rectangular bioactive fibers based on doped and non-doped borosilicate glass constituting the core and the clad of the fiber respectively. The stability of these fibers in aqueous medium is monitored according to the geometry. This study also provides information on resistance to defects depending on the nature of the network and on the development of new bioactive fibers, the emission of which could be used to follow the dissolution of the fiber in aqueous medium. This study contributes to a better fundamental understanding of how composition changes and thermal/radiation processes can modulate the performance parameters of glass materials doped by Yb^{3+} ions.

Keywords: Glass ceramics, ytterbium, bioactive materials

Unité de recherche

ICMCB, UMR 5026 - 87 Avenue du Dr. Schweitzer